DEMOUNTABLE RESISTIVE JOINT DESIGN FOR HIGH CURRENT SUPERCONDUCTORS

Jean-Marie Noterdaeme

Research Report PFC/RR-78-11

October 1978

DEMOUNTABLE RESISTIVE JOINT DESIGN FOR HIGH CURRENT SUPERCONDUCTORS

by

Jean-Marie Noterdaeme

Burgerlijk Werktuigkundig Electrotechnisch Ingenieur

Rijksuniversiteit Gent, Belgium

1977

Submitted in partial fulfillment

of the requirements for the

Degree of

Master of Science

at the

Massachusetts Institute of Technology

May 1978

© Jean-Marie Noterdaeme 1978

Signature of Author . . . . . .
Department of Nuclear Engineering, May 12, 1978

Certified by . . . . . .
Thesis Supervisor

Accepted by . . . . . .
Chairman, Department Committee

DEMOUNTABLE RESISTIVE JOINT DESIGN FOR HIGH CURRENT SUPERCONDUCTORS

by

Jean-Marie Noterdaeme

Submitted to the Department of Nuclear Engineering on May 12th, in partial fulfillment of the requirements for the Degree of Master of Science

ABSTRACT

Recent fusion reactor designs show the need for data on the resistance of demountable joints in superconductors. An experiment was set up to measure this resistance at different pressures. The resistance is calculated from the measured decay time of the current in a superconductive loop. This method proved to be much better than the usual volt-ammeter method. Calibrated compression washers were used to provide the pressure. A resistance of $1.5 \times 10^{-9} \Omega cm^2$ was achieved with silverplated joints 24000 psi. Data are provided for other contact materials.

Name of Thesis Supervisor: Lawrence M. Lidsky

Title: Professor of Nuclear Engineering

ACKNOWLEDGEMENTS

This year of study in the United States was made possible by the B.A.E.F. (Belgian American Educational Foundation). I am very indebted to this foundation and I gratefully acknowledge their support.

I would like to thank my professors and especially Professor L.M. Lidsky, my thesis advisor, for the time he devoted to me. My thanks also to Professor Politzer for showing true interest in the experiment.

At the Francis Bitter National Magnet Lab the work was more directly supervised by Dr. B. Montgomery and Dr. Y. Iwasa. Dr. Montgomery helped me to focus on the parameter range the experiment was to be built for. Dr. Iwasa made the equipment for the experiment available and his experience was valuable to me.

Dr. R.D. Hay of the Plasma Fusion Center shared his knowledge on the subject through very interesting conversations.

I am also very grateful to Mr. J. Davis and Mr. Leupold for suggestions about the engineering design of the parts.

My thanks also to the librarians in the M.I.T. libraries, and to Roger, Dick, Mike, Bruce of the N.M.L. for helping to find my way in a new environment.

A special word of thanks to Sheldon Rich who machined with true craftsmanship some parts and gave some very practical hints when I made others. Thanks also to Cathy Lydon for typing this thesis.

DEDICATION

To my parents.

To Michèle

TABLE OF CONTENTS

Table of Contents (continued)

LIST OF FIGURES

LIST OF TABLES

LIST OF PICTURES

CHAPTER 1

INTRODUCTION

A. Background

When Kamerlingh Onnes liquified helium in 1908 and discovered in 1911 the superconductive state of matter he was certainly far from the thought that his pioneer work in low temperature physics might eventually be instrumental in the achievement of the highest temperature on earth. Superconductivity is the property of material in some range of temperature, magnetic field, current density and pressure to loose all resistance. It is not our purpose to go in detail into the phenomenon. In Appendix A some books on the subject are listed together with a brief comment to guide the interested reader. In the next chapter a brief review will be given.

The most widely used material of this moment is NbTi on which some more information can be gathered from (1). Data about the critical current density, in function of temperature and external magnetic field can be found in (2).

Another material which has higher critical current density and can be used in higher fields is Nb_3Sn. The material, however, is brittle and special methods have to be used to make it into useable conductors (3,4).

B. Superconductivity and Joints

While the phenomenon is known for many years, it is only recently that technological applications of superconductivity have appeared. An excellent review article on superconductivity and its application has been written by B.B. Schwartz and S. Foner (5). They report on four main areas of applications: electrical motors and generators; superconducting magnets, including those for magnetohydrodynamic and fusion power generation; power transmission and magnetic levitation for high-speed ground transportation. Focusing more on the fusion power application of superconducting magnet is the article by P. Komareck (6).

When using superconductors for application, one has to be aware of two major limitations.

The first one is the range of parameters at which superconductivity occurs. We will only consider ourselves with atompheric pressures; for tests at higher pressure we refer to (7). At zero field, the change from normal to superconductive state is abrupt and no problem arise in defining a critical temperature and current. In the presence of a magnetic field superconductors behave in two different patterns. (A third pattern, the surface superconductivity does not occur for superconductive material embedded in metal). Type I superconductors go in the general case from the superconductive to the normal state

through an intermediate state in which normal and superconductive regions are intermixed (Fig. 1a). The superconductive regions do not contain any magnetic flux (Meisner effect) while the normal regions do. When we increase the magnetic field the normal regions will grow and the superconductive regions shrink. This intermediate state will not occur and the Type I superconductor will go from the superconductive to the normal state abruptly in the case of a long thick cylinder with parallel magnetic field. For type II superconductors the transition occurs through a so called mixed state (even for a cylinder) where the normal regions form an array of narrow cylinders of material in the normal state surrounded by the remaining superconductive material (Fig. 1b).

In a higher magnetic field the thickness of those normal filaments will not increase but more filaments will be formed. Each normal filament can be seen as the center of a vortex of current. A conduction current through the superconductor will cause the vortex line to move due to the Lorentz force. This motion would cause an electric field, and accordingly the sample has become resistive. However, motion of those lines can be prevented by metallurgical defects which pin the vortex

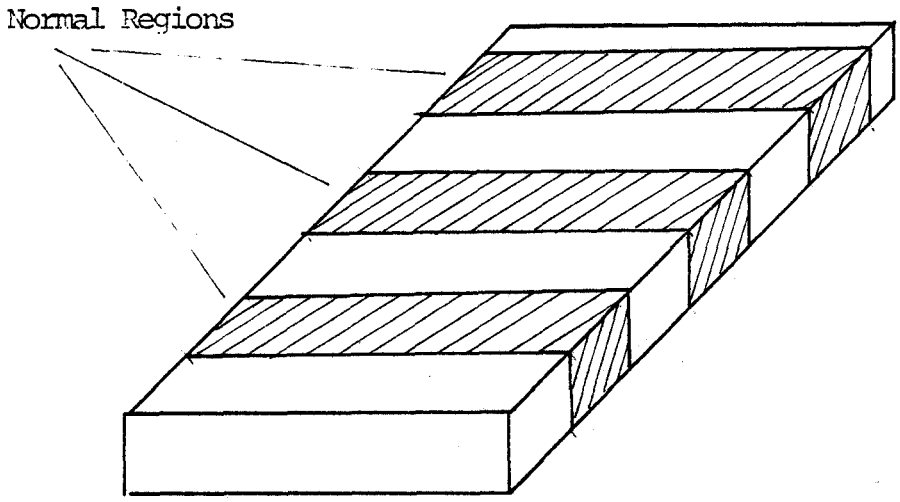

Figure 1a Intermediate State of superconducting Material

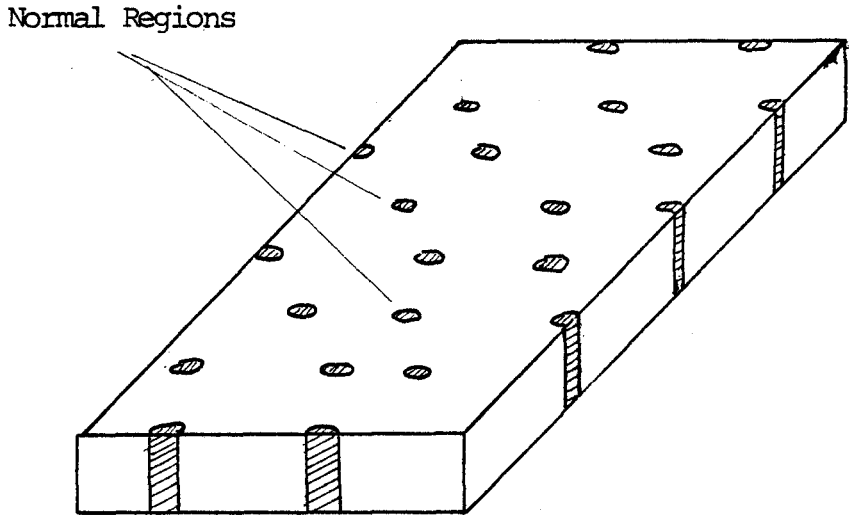

Figure 1b Mixed State of superconducting Material

lines. The sample retains its zero resistance properties up through the critical field H_{c_2} where the transition to total normal state occurs. The domain in which a material is superconductive can be concisely shown in a three dimensional plot. Figure 2 gives the critical characteristics of high field superconductors (taken from Ref. 5).

The transition to normal state can occur inadvertently, due to heat generation by friction, sudden motion of the vortices (flux jump), etc. This would lead to unacceptable catastrophic results in case of magnets with large stored energy. In order to avoid these problems the superconductors are stabilized by dividing the superconductors into fine filaments and embedding it in a matrix of highly conducting normal metal (copper or aluminum). Several approaches are persued (8). In cryostatic stabilization a low resistance path is provided for the current in case some part of the superconductive material goes normal. The cooling is sufficient enough to remove the ohmic heating, to prevent the normal region to extend and the conductor will be brought back to the superconductive state. Cryostatically stabilized conductors are safe against instability due to flux jumping and to mechanical origins (friction). Other stabilization methods provide

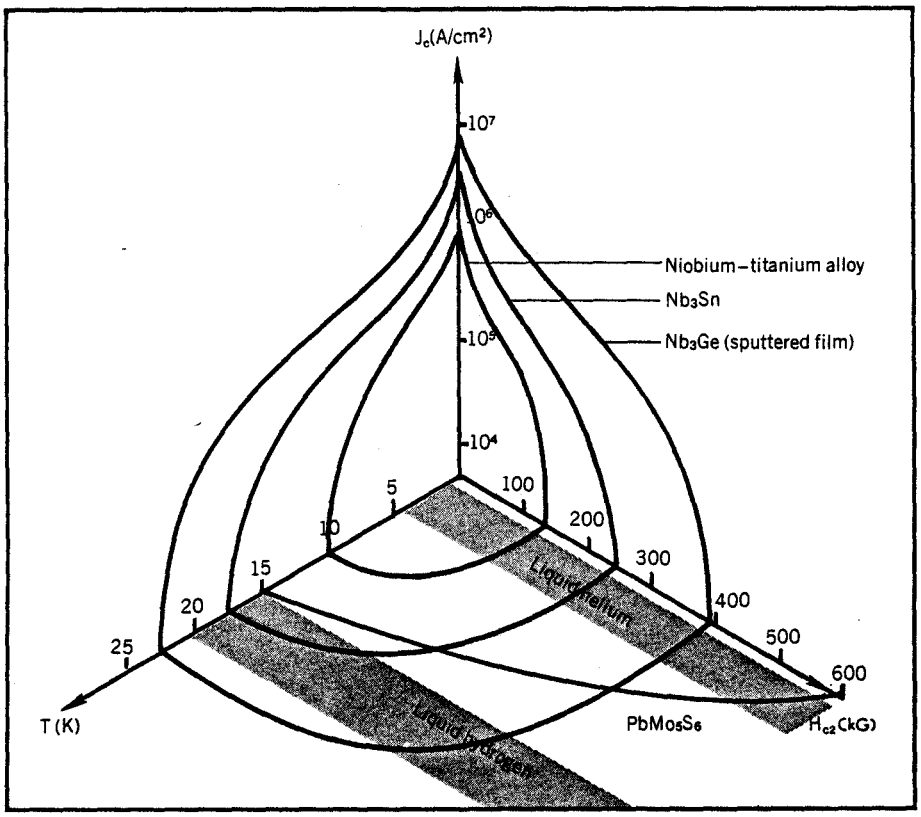

Critical characteristics of high-field superconductors. The critical current density J_c (on a log scale) is shown as a function of the critical upper magnetic field H_{c2} and the temperature T for three readily available superconductors. A plot of H_{c2} versus T is also shown for the ultrahigh-field compound $PbMo_5S_6$. (After J. R. Gavaler and S. Foner.) Figure 2

stability against flux jumping but not against mechanical instability. They rely on the fine subdivision of the superconductor and on the embedding in a metal. The high thermal conductivity of the metal prevents a local flux instability to grow by removing the heat fast enough (adiabatic stabilization). The high electrical conductivity magnetically damps the motion of the vortices so that more time is allowed for heat conduction (dynamic stabilization).

The solution of this problem brings about the second limitation. Due to technological factors in the manufacturing, the superconductor are available in limited length only. If longer lengths are required, one has to come up with an acceptable way of making joints. A good state of the art in joint design is given in (9). Depending on the specific applications, some required characteristics of joints will be more emphasized than others. The report lists 6 basic characteristics.

1. Compatibility with cryogenic environment,
2. Strength,
3. Electrical characteristics,
4. Ease of fabrication,
5. Ease of inspection,
6. Cross-section dimensions.

Depending on the types of conductors to be joined, and the required characteristics,different bonding techniques and joint designs will be used. Where very low resistance is important and increased cross section a minor disadvantage one tries to come as close as possible to superconductor-superconductor contact by cold pressing of twisted superconductor wire in a metal sleeve (10), sometimes after stripping them first from the stabilization material (11). Other methods are spot welding (12,13), or butt welding (14). In the case a continuous cross section is given the priority, a scarf joint will be the candidate joint design. As bonding techniques we list ultrasonic welding (15), explosive welding (16). Electron beam welding, laser welding, are more advanced methods. Various types of soft solder, with different joint designs (lap, lap with reinforcement, scarf joint) give good results and have the advantage of easy fabrication (17). There are, however,other cases where it is not limited length of the superconductor which brings about the need of making a joint. In those cases other characteristics than listed above will be required. A switch between the terminals of a superconducting coil is necessary to allow its use in the persistent mode. For small coils the switch is constructed of a superconductor

which can be in its normal state (during the charging of the coil) and in its superconductive state (for the persistent mode). For large coils the energy losses during the charging process would be too high so that an actual disconnect is desirable (18,19). Requirements for those kind of switch are low resistance, ease of opening and closing the switch, withstanding of a sufficient number of switching operation, reliability (19). When very low resistance, rather than a compact switch is the goal special multilam louvered bands are used with success.[20] In between the permanent joint and the switch we have demountable joints. This area seems to be very little explored and is the main topic of our thesis.

C. Demountable Joints

There are some specific applications where semi permanent joints are the type of joint that would best be suited. The joint is essentially made to carry current and its ability to be demounted is primary for non-electrical reasons (unlike the switch where the main reason is an electrical one).

A typical application is the removing of the current leads that charged up a superconducting magnet. These current leads present a very high heat input due to the good thermal conductivity and the connection with the outside world. Although part of the problem was circumvented by

by special designs (vapor cooled leads, allowance of a low thermal gradient) the problem would be circumvented altogether if the leads could be removed. Steady state magnets for mirror fusion machines would very much benefit from such a development.

Another application appeared as the likelihood of modular design of toroidal machines became more evident. In this application it is mainly the removal of the mechanical link that the superconductor achieves between the different modules that is the sought after property of the demountable joint.

The demountable joint is a type that has its own requirements different from the permanent joint and the switch. For a permanent joint very often the space allowance is quite strict, the low resistance, however, can be achieved by increasing the contact area (scarf joint) and very intimate bonding between the two surfaces. For a switch the lesser bonding is compensated by more freedom on the space allowance. A demountable joint doesn't have the generous space allowance of the switch nor the very intimate bonding of the two surfaces. This is the dark side. But it is not all bad. As the joint doesn't have to be switched frequently and rapidly, more rugged mechanical devices can be used and higher pressures applied.

The mechanical strength doesn't have to be provided by the joint itself, as in the permanent joint, but can be supplied through the support that provides the pressure. In the next chapter, when discussing our results we will have to compare our results with data from soldered joints and switches.

CHAPTER 2

THE MEASUREMENT OF SMALL RESISTANCE

A. General

Every relationship containing R, the resistance is a potential basis for a method to measure the resistance. Three come easily to mind. The usual ohms law, $V=RI$, is the basis of several methods, which are used for a wide range of resistance measurements. The relation $P = RI^2$ could be another basis. Measuring the power dissipated could allow to measure the resistance for a known current. Induction methods is the general name for the third series of methods. For low resistance (we are speaking of the order of $10^{-8}\Omega$), of course, great care has to be taken in applying those methods: Contact resistance can be of the order of $10^{-3}\Omega$.

The first method[21] developed into:

1. The volt and ammeter methods, where the voltage drop across potential taps is measured for a known current through the samples. This is the most widely used method but gives often rise to problems (the voltage to be measured are of the μV range).

2. The potentiometer method; the low resistance is compared with a standard resistance of the same order magnitude. Those standard resistances, however, are only

available to 0.0001Ω.

3. Several bridge methods are reported. The Kelvin Double Bridge is less suitable for low temperature work since the thick copper leads that are essential for its use provide a high terminal input (22).

The second method is rather theoretical than practical at these power levels. For 1000A and $10^{-8}\Omega$ the power boils off $4x10^{-3}$ cm^3 liquid helium per second. This is a volume of approximately 2.5 cm^3/sec of helium gas at room temperature and pressure.

The third method, although in recent years superceeded by the volt and ammeter method, because of its convenience is actually the most suitable one for low resistance,measurements. Induction methods have definite advantages. One very important advantage is that no large current carrying leads have to be brought down into the dewar. However, as Meaden[22] writes "electrodeless induction methods have not as yet proved very popular for purposes of resistance measurement. This is perhaps because they are essentially comparison methods and do not always give the resistance directly and simply. In some cases, also, the auxiliary equipment is rather elaborate, and possibly the procedure is considered laborious". For resistances lower than 10^{-10} this method is the only available one. Three distinct approaches are feasible of which two are mainly designed for bulk material resistivity measure-

ments.

The introduction of an electrical conductor into the field of an inductor modifies the resistive and inductive components of the inductance. From this the resistivity of the sample can be calculated (23).

The second approach is that of the rotating magnetic field (24). The conductivity of the specimen is determined from the magnitude of the torque on the specimen by the rotating magnetic field.

A method that can be used for bulk materials as well as for loops is the eddy current method for measuring the resistivity of metals. For bulk materials the method is described in (25). The method can also be used for loops. As this is the approach that was persued a more detailed description is given in the next paragraph.

B. Persistent Current Decay Measurement

With this method the resistance can be easily calculated from the decay rate of a current in a loop and the knowledge of the inductance of that loop. Lenz's law states that

$$-\frac{d\Phi}{dt} = RI + L\frac{dI}{dt}$$

$$\Phi = \iint \bar{B} \cdot d\bar{S}$$

R resistance of the loop

I current in the loop

L inductance of the loop

Φ flux due to external magnetic fields

$\overline{B}$ external magnetic field

t time

$d\overline{S}$ surface element. The integral is performed over any surface that has the loop as its boundary. The unit vector on the surface is chosen in accordance with the direction of current and the right hand rule.

Suppose the external magnetic field is kept zero, or a constant, and that the current at some initial time is $I = I_o$. Then the solution of the equation is given by $I(t) = I_o\, e^{-t/\tau}$ where $\tau = \frac{L}{R}$ is called the time constant of the system. On semilog paper the equation is a line $\ln I = \ln I_o - \frac{t}{\tau}$ from which slope, the time constant τ can be measured. The inductance L of the loop can be measured or calculated (we will go into more detail when describing the experiment). The resistance then follows easily from $R = \frac{L}{\tau}$.

Onnes was the first one to use the method in 1914. More recently the method was used by Iwasa (26). As men-

tioned before the method is used mainly for extremely low resistance measurements ($10^{-14}\Omega$). For our experiment, preliminary calculations based on data on the resistance of soldered joints and switches made clear that for suitable choice of the surface area of the joint and the inductance of the loop, we could achieve very comfortable time constants in the range of 2 to 200 sec for range of two decades of resistance values in the expected range.

The measurement of the decay rate of the circuit can be done in several ways. A Hall probe can be used which measures the magnetic field of the current in the loop. Another way is using a Ragowski coil. Integrating the output of the coil gives at any time the current through the loop. When the time constant of the system is large drift of the integrator can become a problem. The current can be measured at time intervals by moving a search coil in the field of the loop and integrating the output from zero field to maximum field.

We used a fixed search coil; its voltage or integrated voltage, depending on the situation, was recorded. Let us clarify the behavior of the system. The numbers 1, 2, 3 in Figure 3 refer respectively to the external magnets, the superconductive loop and the search coil. We use as notation L_i for the self inductance of the coil i and M_{ij} for the mutual inductance between coil i and j. With the

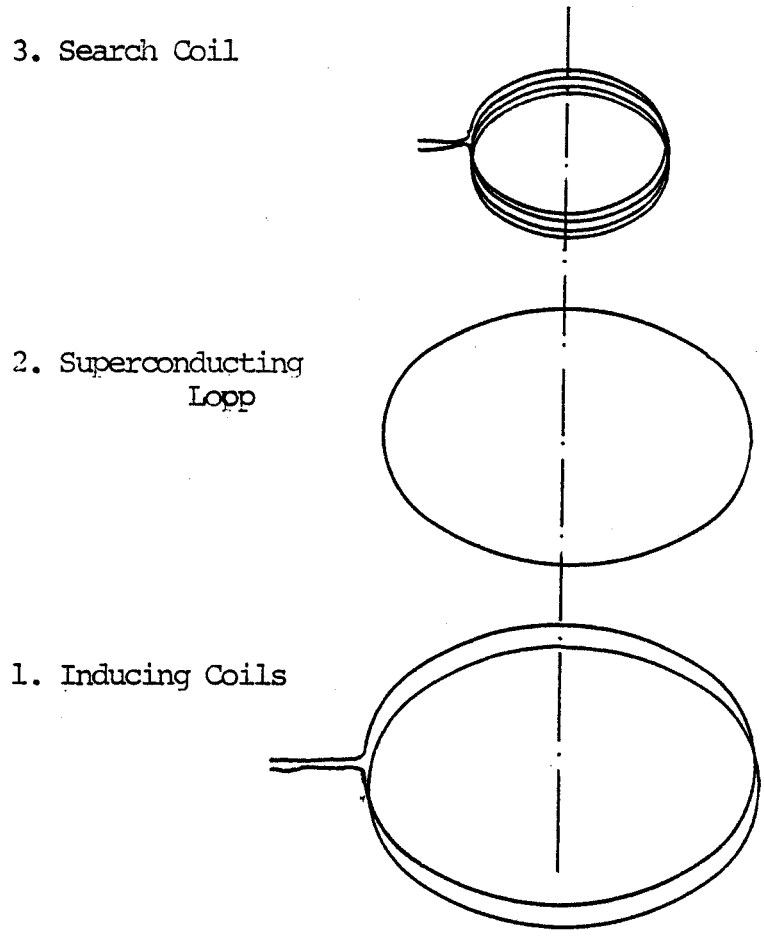

Figure 3. Schematic Representation of the Magnetic Circuit.

correct sign of the mutual inductances the circuit is governed by the following equations:

$$V_1 - R_1 I_1 = L_1 \frac{dI_1}{dt} + M_{12} \frac{dI_2}{dt} + M_{13} \frac{dI_3}{dt}$$

$$V_2 - R_2 I_2 = M_{12} \frac{dI_1}{dt} + L_2 \frac{dI_2}{dt} + M_{23} \frac{dI_3}{dt}$$

$$V_3 - R_3 I_3 = M_{13} \frac{dI_1}{dt} + M_{23} \frac{dI_2}{dt} + L_3 \frac{dI_3}{dt}$$

Those equations can be simplified in the following way. The search coil 3 is connected to a high impedance amplifier so that no current is flowing $I_3 \equiv 0$. The loop 2 is closed so that there is no terminal voltage $V_2 \equiv 0$. Let us further consider ourselves only with the last three equations

$$M_{12} \frac{dI_1}{dt} + L_2 \frac{dI_2}{dt} + R_2 I_2 = 0$$

$$V_3 = M_{13} \frac{dI_1}{dt} + M_{23} \frac{dI_2}{dt}$$

We can distinguish between two periods. First when the change of current in the external coils creates a changing flux, thus inducing a current in the loop 2 and a voltage in the search coil 3. Second when there is no

change in external magnetic field and the current in 2 decays exponentially. We look at the first case. If we assume $\frac{dI_1}{dt} = - C$

$$M_{12}C = L_2 \frac{dI_2}{dt} + R_2 I_2$$

Solution

$$I_2(t) = \frac{M_{12}C}{R_2} (1-e^{-t/\tau}) \text{ with } \tau = \frac{L_2}{R_2}$$

Let t_o be time at which the current in the external solenoid 1 becomes and remains zero. This time was much lower than the time constant τ (this is not true in case the current carrying velocity of the joint is exceeded. This was never the case). Thus $I_2 = \frac{M_{12}C}{R_2} (\frac{t_o}{\tau})$; with $C = \frac{I_1(o)}{t_o}$ and $\tau = \frac{L_2}{R}$, we have that $I_2(t_o) = \frac{M_{12}}{L_2} I_1(o)$. In the same approximation

$$V_3 = \frac{I_1(o)}{t_o} [-M_{13} + \frac{M_{23} M_{12}}{L_2}]$$

$$\int_o^t V_3 \, dt = \frac{I_1(o)}{t_o} [-M_{13} + \frac{M_{23} M_{12}}{L_2}] t$$

During the second period

$$L_2 \frac{dI_2}{dt} + R_2 I_2 = 0$$

$$V_3 = M_{23} \frac{dI_2}{dt}$$

with $I_2(t_o) = \frac{M_{12}}{L_2} I_1(o)$

Solution:

$$I_2 = I_2(t_o)\, e^{-(t-t_o)/\tau}$$

$$V_3 = -M_{23} \frac{R_2}{L_2} I_2(t_o) e^{-(t-t_o)/\tau}$$

$$\int_o^t V_3 dt = -M_{13} I_1(o) + M_{23} I_2(t_o) e^{-(t-t_o)/\tau}$$

Figure 4 gives an idea of those solutions, with t_o much exagerated compared to τ. Recording the voltage from the search coil gives us immediately the time constant of the system. The current that was induced in the loop can be calculated from

$$I_2(t_o) = \frac{1}{M_{23}} \left[- \int_{t_o}^{\infty} V_3 dt \right]$$

This is the correct result, even without the made approximation. Now that the theoretical basis is laid we can be more specific about the experiment itself.

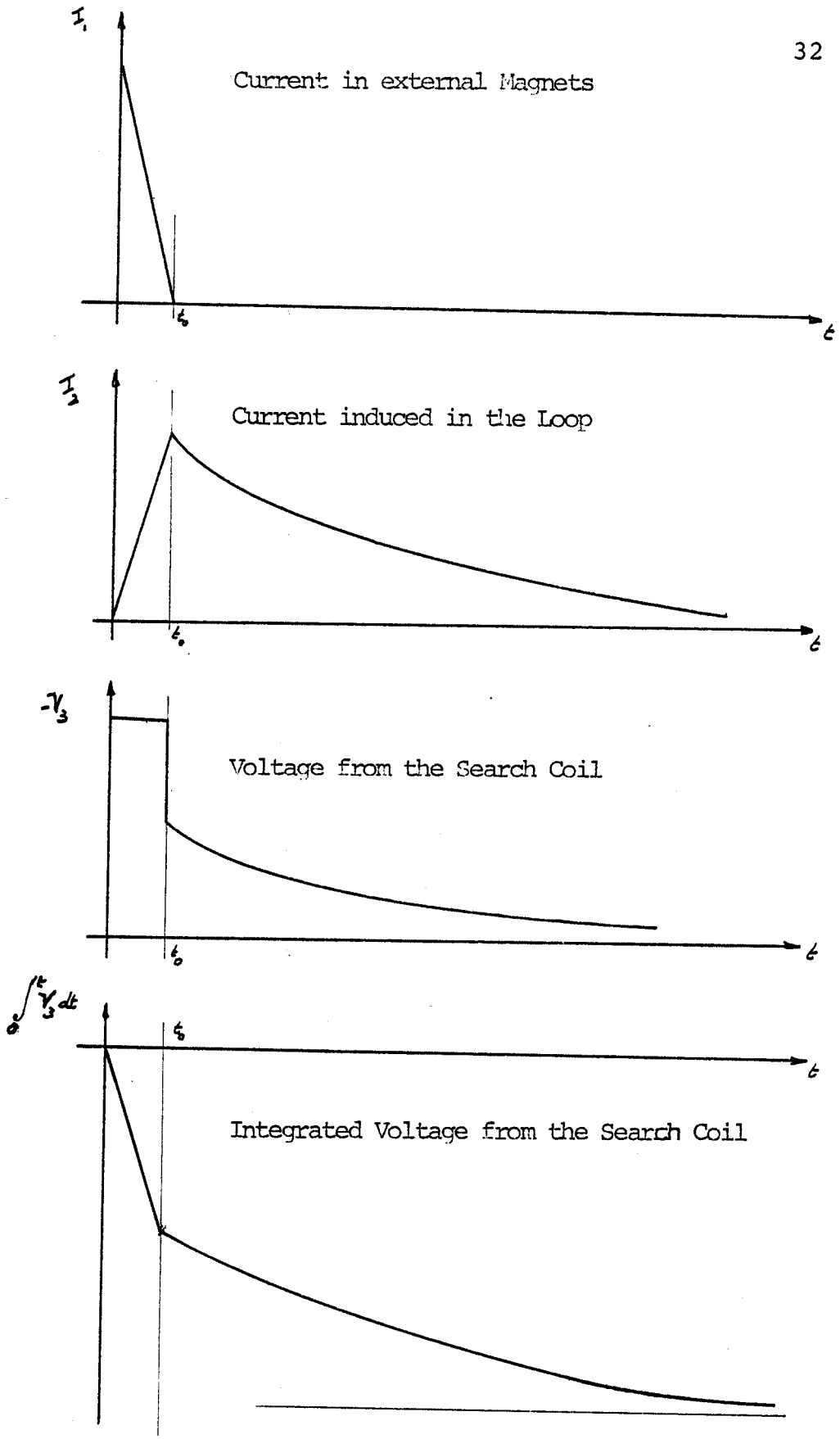
I_1
Current in external Magnets
t_0
t
I_2
Current induced in the Loop
t_0
t
$-V_3$
Voltage from the Search Coil
t_0
t
$\int_0^t V_3\,dt$
t_0
t
Integrated Voltage from the Search Coil

Figure 4.

CHAPTER 3

THE EXPERIMENT

A. The Experimental Set Up

From the theory in the previous chapter it is clear that there are three main parts, the external magnet, the sample holder, and the search coal. These will be discussed separately after the reader has been familiarized with the complete set up.

Figure 5 gives an overall view of the experiment. The scale is 1/10. The two external solenoids, connected in series, encircle the bottom of the deward. The sample holder is suspended in the dewar by a 1/2" stainless steel rod. Two more stainless steel rods are used to provide a passage through the insulation material for the wires and for the dip stick (stick used to measure the liquid helium level). The search coil itself, not visible in Figure 5 is located inside the sample holder; this will become clearer after the explanation of the holder. The dewar was supported by a wooden frame.

The two external magnets are commercially available solenoids (Alpha Scientific Laboratories, Inc. , Model Solenoid Coils, Serial No. 732/3340-1 and no. 732/3340-2). Internal Diameter 6 inches, External Diameter 14 inches, thickness 2 1/4 inches. Both magnets were cooled with water (in series), the lower one was supported by an aluminum

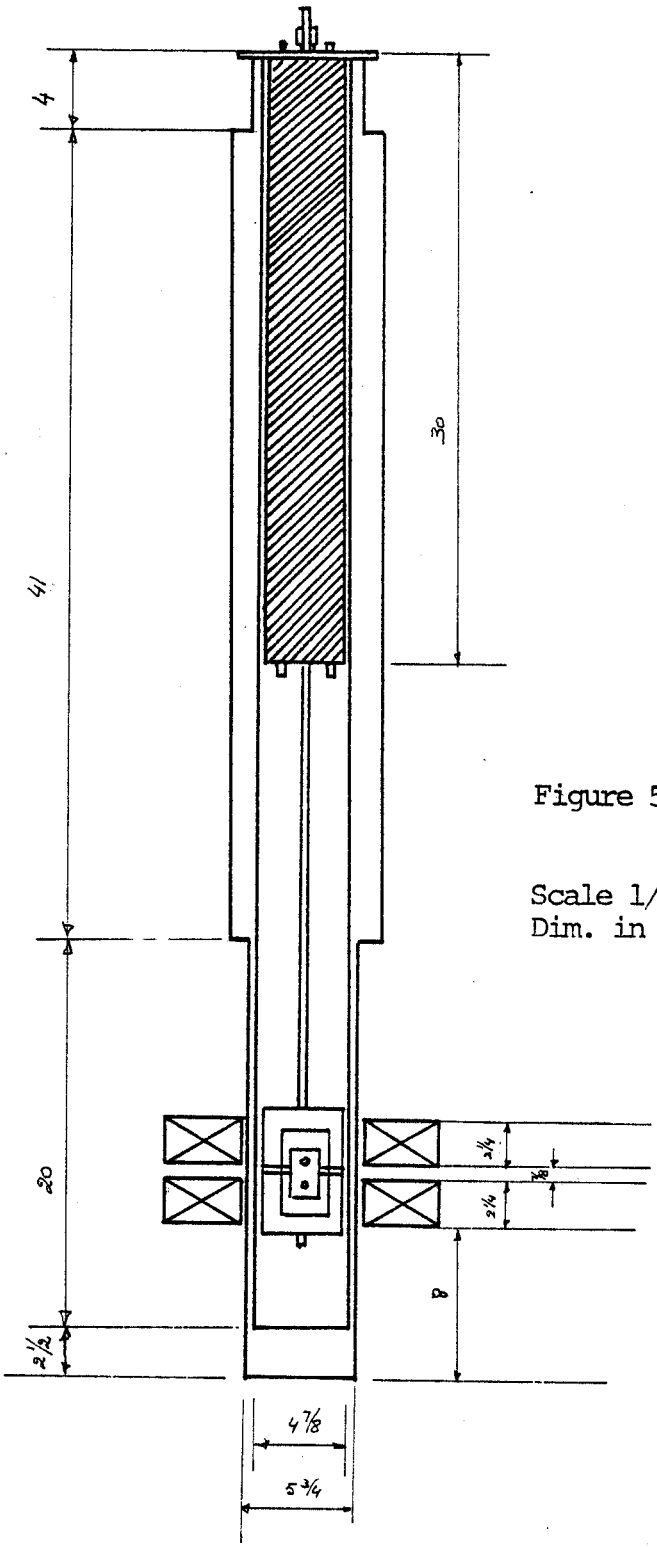

Figure 5.

Scale 1/lo
Dim. in inches

cylinder, while the upper one rested on a wooden support which at the same time provided the spacing between the two magnets.

Figure 6 clarifies the design of the sample holder. The superconductive loop is supported by a thin walled cylinder of phenolic. Grooves in this cylinder secure the ribbon. The tube is partly cut out in order to support a 3/8" thick, flat stainless steel plate, again with grooves. A second plate can be bolted to the first one with two 1/2" bolts. The ribbon is led around the cylinder in the grooves. The joint is made by overlapping the two ends of the loop and clamping them between the two stainless steel plates. Two type of joints can be made. Figure 7 explains schematically the location of the grooves for the two types of joints.

The pressure applied on the joint can be adjusted by using one or more calibrated stainless steel compression washers. Solon stainless steel compression washers #8-M-89301 were used for this purpose.

Inner Diameter: 33/64"

Outer Diameter: 1 - 3/16"

Material Thickness: 0.089"

Deflection (flat): 0.023"

Load (flat): 2600 lb.

Type 301 stainless steel.

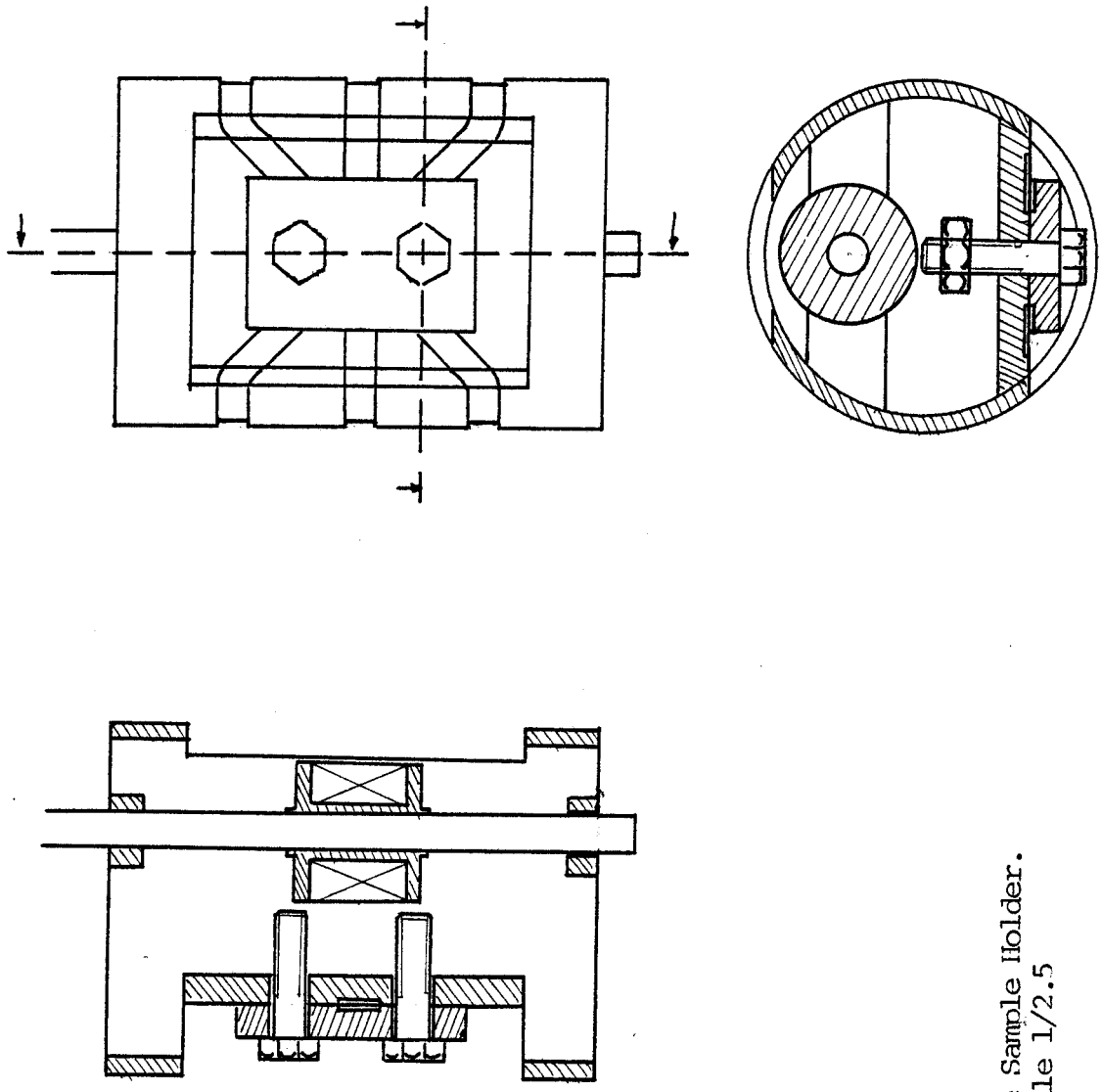

Figure 6. The Sample Holder.
Scale 1/2.5

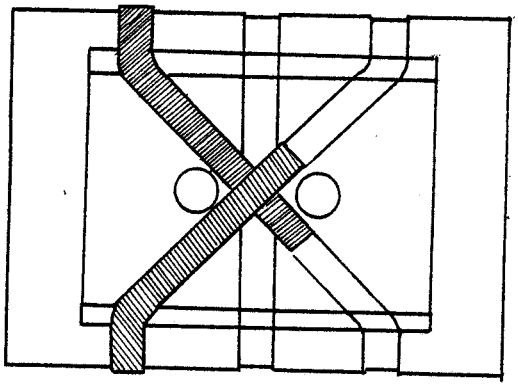

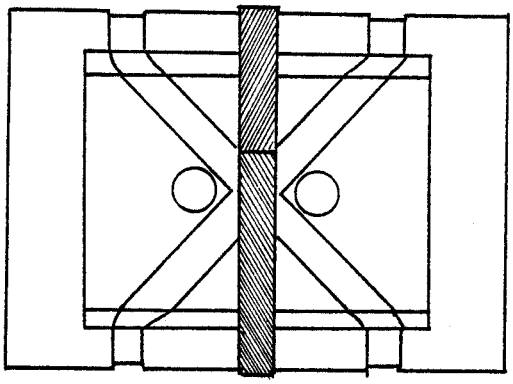

Figure 7. two types of Joint.
(superconductor shaded, top plate removed)

The stainless steel rod which supports the sample holder and the search coil is soldered to the brass piece at the top of the holder. The fitting in the brass piece at the bottom is a free fitting. This way it was possible to work on the sample holder alone, whenver needed (for example to put in a new sample, or to change the pressure). By unscrewing the four screws that attach the upper brass support to the plastic tube and sliding the stainless steel tube out of the lower brass holder, we can completely separate the sample holder from the rest. The upper brass support, as well as the search coil remain attached to the tube. More room is now available inside the tube to bolt and unbolt the nuts and the delicate search coil can remain in a safe place.

Figure 8 is a more detailed view of the search coil. The search coil was made of 45000 turns of #40 wire. Diameter 3.145 mills at 20°C. Resistance at 20°C 1,049.0Ω per 1000 ft. Weight 0.02993 lb. per 1000 ft. The wires connecting the search coil to the amplifiers were a twisted pair of #24 wire. The total resistance was measured to be 19kΩ of room temperature.

B. The Measurements

1. Magnetic Field

First the field produced by the magnets was measured. Ten amperes d.c. was put through the coils (in series). A

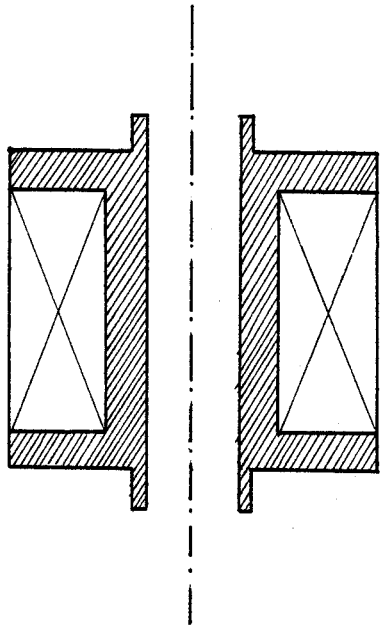

Figure 8. Search Coil.
Scale 1/1

Hall probe was used to measure the field, the Hall probe was connected to a qaussmeter with digital read out. To locate the probe precisely in the Dewar (horizontally as well as vertically) we put it in a stainless steel tube which was held in position inside the Dewar by means of two quard rings, one at the top, in which the tube could slide, and one at the bottom, attached to the tube, sliding in the Dewar. Figure 9 gives the result on axis, the distance is measured from the inner bottom of the Dewar. At the left the location of the coils is indicated schematically.

2. Calibration of the Inductances

2.1 Self-Inductance of the Loop

Let us first consider some data about the loop. The ribbon was made by magnetic corporation of America

size .394"x.035"

W.O. No. M14-19

Billet No. 460

Cu-Superconductor Ratio 2.6/1

Filaments 132

Twist 1.2 turns per inch

No insulation.

A typical cross section can be seen in Picture 1. Picture 2 shows an S.E.M. photograph of the surface, magnification 5000.

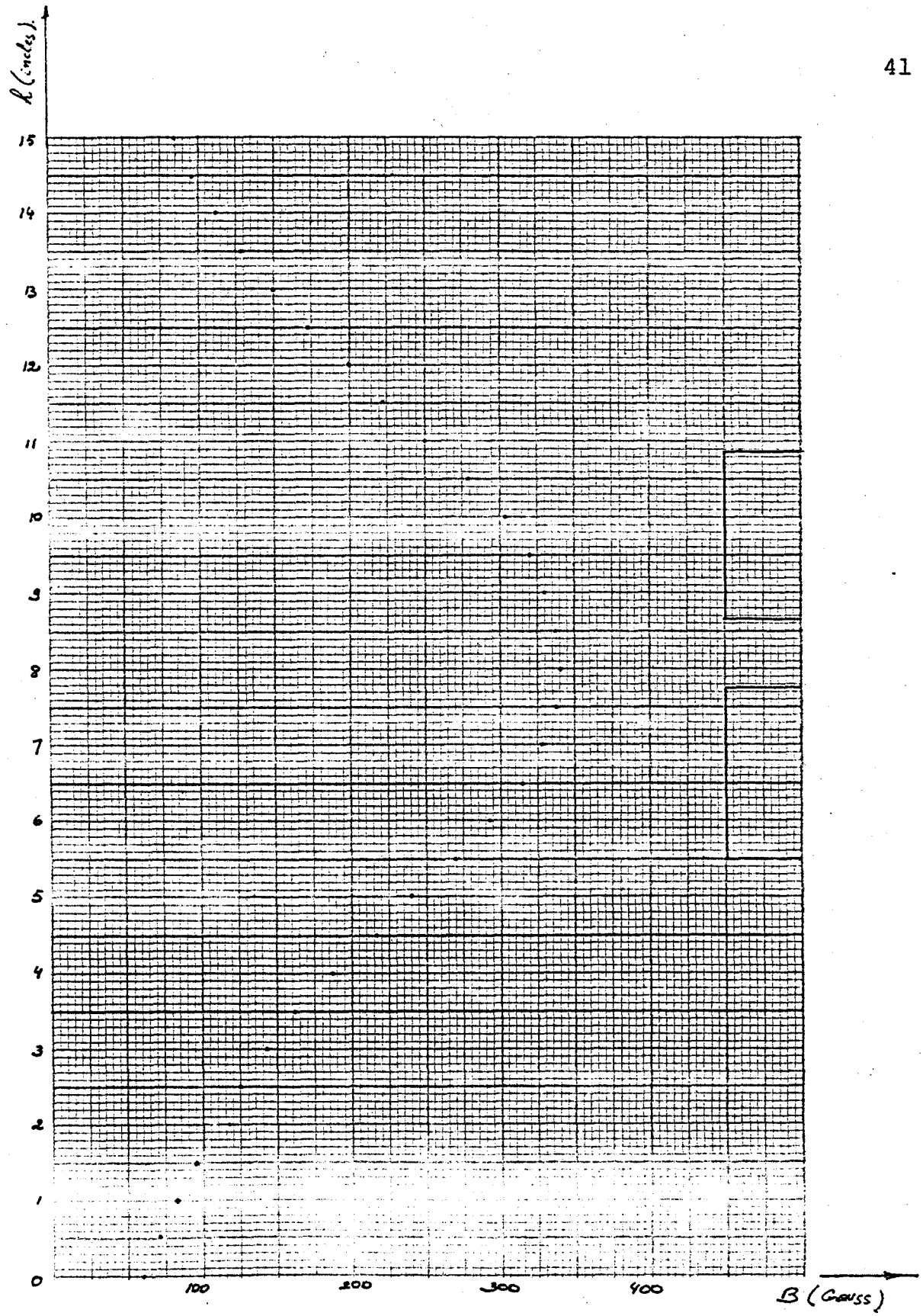

Figure 9. On Axis Magnetic Field.

TECHNOLOGY STORE, M. I. T.

Picture 2. Copper Surface. (5000X)

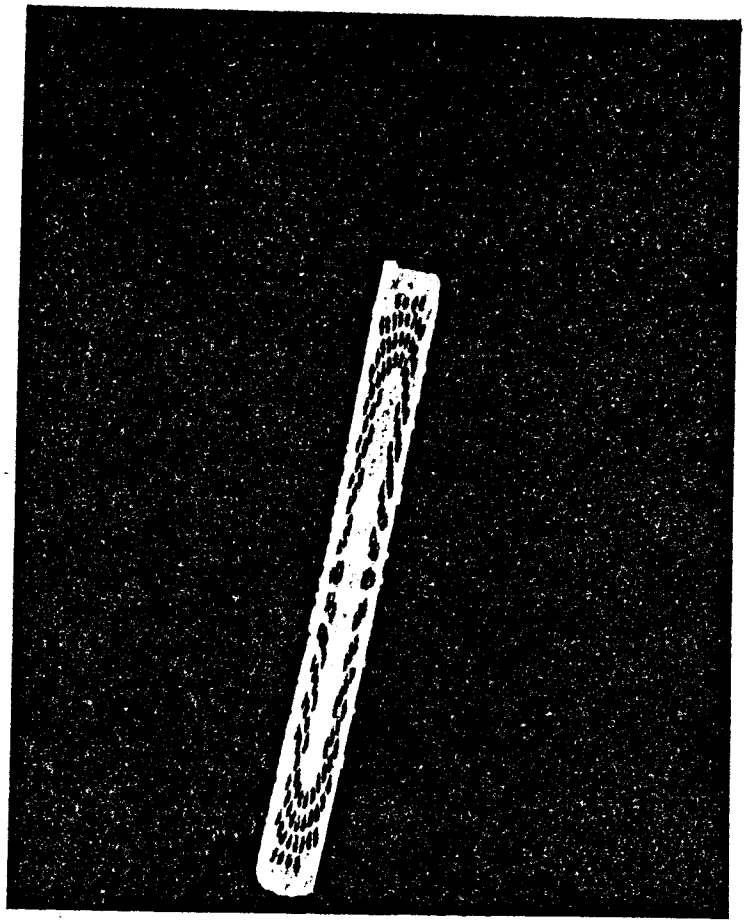

Picture 1. Cross Section of the Superconductor.

The white band at the bottom is 10μm long. Pictures 3 and 4 show in more detail the cross section (those two pictures were made from the ends of sample #12). The magnification is 50X.

The reader will remember that the loop was D-shaped (flattened where the joint was clamped between the plates). An exact calculation of the inductance would be much too complicated. Calculations were made in several idealized cases.

One filament can be approximated by a wire of elliptical cross section, with 2a = 0.0325 cm and 2b = 7.5×10^{-3} cm. The inductance of one filament is, for a circular loop with as radius the radius of the circular part of the real loop, 4.9×10^{-7}H. If all the filaments were perfectly coupled the inductance for the 132 filaments would also be 4.9×10^{-7}H.

The inductance for a circular loop, with a rectangular cross section, and distributed current is 1.0×10^{-7}H.

The inductance was finally measured with a Wayne Kerr Bridge. (Universal Bridge type B 221A Serial No. 1814). The design of the bridge is based on the transformer ratio arm principle. A full explanation of the theory of operation is given in Wayne Kerr Monograph No. 1, "The transformer Ratio-Arm Bridge" available on request from the Wayne Kerr Laboratories Limited, Chessington Surrey, England. The normal range of the transformer bridge ex-

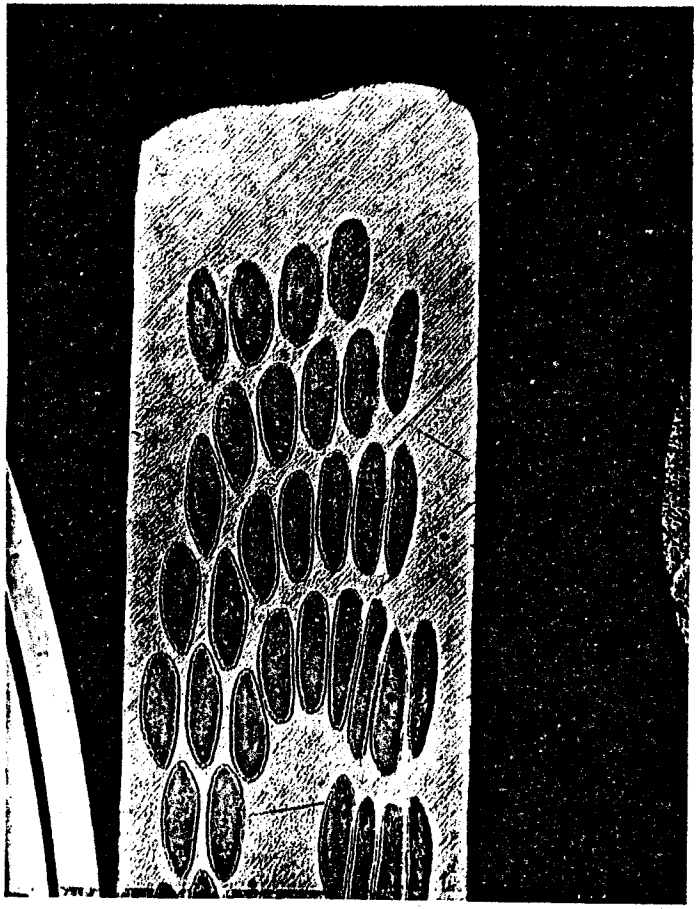

Picture 4. End part of Cross Section (50X)

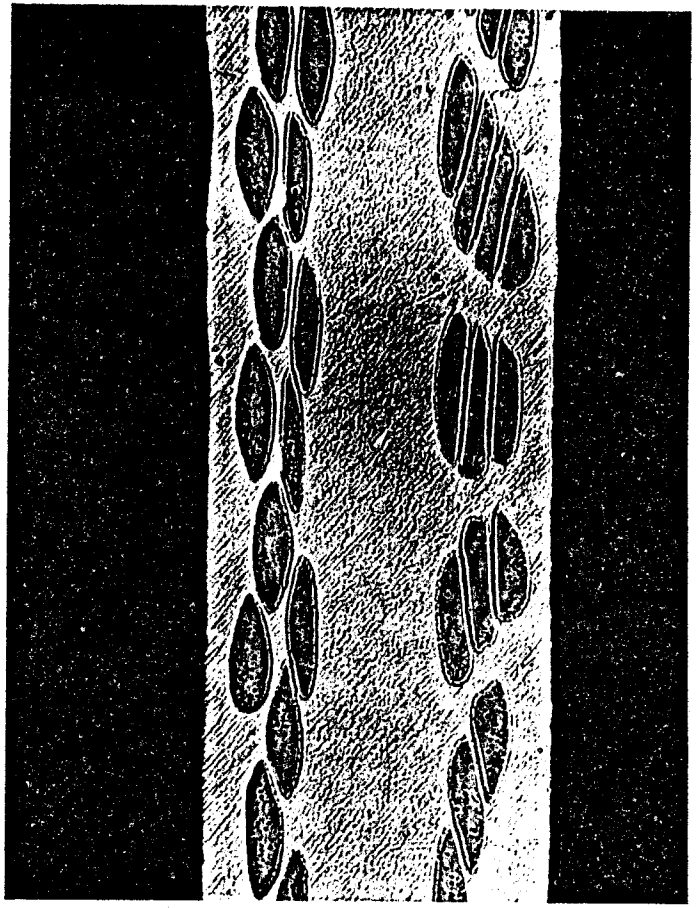

Picture 3. Middle part of Cross Section (50X)

tends down to L = 0.9mH. A low impedance adaptor, however enables us to measure inductances as low as 1×10^{-8}H. For certain choice of settings on the bridge and on the adapter different ranges can be selected. The measurements were made at $\omega = 10^4$ cycles/sec. The skin depth at this frequency is $\delta = \sqrt{\frac{2}{\omega\mu\sigma}} = 1.5$mm. Recall that the ribbon is 10mm x 0.9mm. At this frequency the distribution of the current will be close to the current distribution in the superconducting state. We first measured a calibrated inductance of 15×10^{-7}H to check the procedure, then the inductance of the loop was measured, the leads were as short as possible (2 cm) and twisted. The range 0 - 1μH (bridge on range 5, C on 0.1 and adaptor on range 1) was used with the first division at 0.02μH. The measured inductance was 2.0×10^{-7}H. The bridge could be equilibrated within 0.1×10^{-7}H. Then, with similar leads the inductance of a piece of wire 3cm long, ϕ 1.5mm was measured and was within the measurement error. The contributor of the leads can thus be neglected. For the calculation of the resistance the measured value of L = 2.0×10^{-7}H was used.

2.2 The Mutual Inductances

From the end of the second chapter it is clear that M_{23} has to be known, in order to be able to calculate the induced current from the formula

$$I_2(t_o) = \frac{1}{M_{23}} \left[- \int_{t_o}^{\infty} V_2 dt \right].$$

The mutual inductance M_{23} between the loop and the search coil is completely fixed by the geometry of the sample holder with the search coil, and independent of its position relative to the external magnets. M_{23} is thus really invariant. The mutual inductances M_{13} and M_{12} depend on the position of the sample holder relative to the external magnets. The sample was very precisely located for the calibration at the maximum of the magnetic field. M_{13} was measured to check the design of the search coil and M_{12} can be used to have an idea of the maximum current that can be induced with the formula $I_2(t_o) = \frac{M_{12}}{L_2} I_1(0)$.

In order to measure M_{23} a dummy sample was made. Rather than making a joint in the loop, the two ends where insulated from each other, leads were connected and brought up outside the Dewar. We put 1A through the loop, interrupted the current and integrated the voltage from the search coil.

$$V_3 - R_3 I_3 = M_{13} \frac{dI_1}{dt} + M_{23} \frac{dI_2}{dt} + L_3 \frac{dI_3}{dt}$$

$$- \int V_3 dt = M_{23} \times 1A.$$

The voltage was integrated with a voltage to frequency con-

verter and a counter with digital display.

To measure M_{12} the same dummy sample was used. However, now the current was put through the external magnets, interrupted, and the voltage induced in the loop was integrated

$$V_2 - R_2 I_2 = M_{12} \frac{dI_1}{dt} + L_2 \frac{dI_2}{dt} + M_{23} \frac{dI_3}{dt}$$

$$- \int V_2 dt = M_{12} \times 1A.$$

The measure M_{13} no sample was inserted and a 1A current through the external coil was interrupted. The voltage from the search coil was integrated.

$$V_3 - R_3 I_3 = M_{13} \frac{dI_1}{dt} + M_{23} \frac{dI_2}{dt} + L_3 \frac{dI_3}{dt}$$

$$- \int V_3 dt = M_{13} \times 1A.$$

This method gives the correct inductances independent of any additional closed loop (like the Dewar for example). Indeed the current in such a loop is zero before the change of the magnetic field, and dies out for $t \to \infty$ so that any additional term $M_{ij} \frac{dI_j}{dt}$ will not contribute after integration. A Hall probe was located in the plane of the sample so that the sample holder could be lowered exactly

to the point of maximum filed of the external coils.

We obtained

$$M_{12} = 4.0 \pm 0.5 \times 10^{-5} \text{ H}$$

$$M_{23} = 6.0 \pm 0.5 \times 10^{-4} \text{H}$$

$$M_{13} = 0.15 \pm 0.02\text{H}.$$

That M_{12} agrees with the calculation can quickly be verified. The field on axis for 10A through the coil 1 is maximum 340G = 0.034T. The area of the loop is approximately $100\text{cm}^2 = 0.01\text{m}^2$. Using $\Phi_{12} = M_{12}I_1 = \int\int_{\text{surface 2}} \bar{B}_1 \cdot d\bar{S}_2$, yields for the mutual inductance $M_{12} \simeq \frac{1}{I_1} \times B_1 \times S_2$ or $M_{12} = \frac{1}{10} \times 0.034 \times 0.01 = 3.4 \times 10^{-5}\text{H}$. The difference being due, of course, to the fact that the field on axis is smaller than in the rest of the plane.

M_{13} can also be calculated. An average area is 10cm^2 and we have 45000 turns. Thus $M_{13} = \frac{1}{10} \times 0.034 \times 10\text{x}10^{-4} \times 45000 = 0.153\text{H}$. A way to check M_{23} is using

$$V_3 = - M_{23} \left(\frac{1}{\tau}\right) I_2(t_o)\, e^{-(t-t_o)/\tau}$$

At $t=t_o$

$$V_3 = - \frac{M_{23}}{t} I_2(t_o)$$

where $I_2(t_o)$ can be estimated from

$$I_2(t_o) = \frac{M_{12}}{L_2} I_1(0).$$

Take, for example, Figure 10 , which is the recorded voltage of the search coil for a typical data point

$$V_3 = - 2.7 \times 10^{-3} V$$

$$t = 200 \text{ sec.}$$

The calculated value of $I_2(t_o)$ = 1000A. So that we can calculate V_3

$$V_3 = - \frac{6.0 \times 10^{-4}}{200} \times 1000 = - 3.0 \times 10^{-3} V.$$

The agreement of the calculated value with the measured is a check for M_{23}.

3. Behavior of the Ribbon Under Pressure

In order to check the behavior of the ribbon under different pressures, two samples of ribbon approximately 5cm long, were laid one above the other at an angle of 90° and pressed together. The contact area is then 1 cm^2. The following table gives an overview of our findings. Note that the yield strength (0.2% Y.S.) of NbTi is approximately 68000 psi (1) and the yield strength of copper is in the range 10000 to 26000 psi. The pressure was applied and removed immediately. One sample was subjected to the pressure of 19400 psi for 2 hours and did not show any dif-

TABLE 1. BEHAVIOR OF THE RIBBON UNDER PRESSURE

Applied Force (kg)	Pressure (psi)	Comment
12000	77500	Thickness reduced, large lateral flow of the copper. Definite impression marks. The superconductors gives a pattern at the contact surface.
9000	58000	Light pattern at the contact surface, light lateral flow of the copper, marks on the copper by the pressure plates.
6000	38700	Pattern only at the sides of the contact surface, light lateral flow, marks on outer surface.
5000	32300	Same pattern, no lateral flow, marks on outer surface.
4000	25800	idem
3000	19400	idem
2500	16000	idem
2000	12900	No more pattern at contact surface only slight marks on the outer surface.
1500	9700	Slighter marks on the outer surface.
1000	6500	No marks on the outer surface.

ference with the sample where the pressure was removed immediately.

4. Measurements of the Resistance

4.1 Soldered Joint

Our first sample was a soldered joint to check the proper operation of the whole system. The voltage from the search coil was amplified and recorded on a x.y recorder with the time in the x direction and the amplified voltage in the y direction. The charts were numbered in sequence, the scales were written down, as well as the current in the external coils. Figure 10 is not from the soldered joint (it is from sample No. 4), but is representative for those cases in which the voltage was recorded. In (a) we located the pen, and in (b) we traced the zero line. The voltage oscillations in (c) are due to the fact that the current, although regulated, still has some ripple. In (d) the current in the outer coil was interrupted, giving at first a very high voltage (out of scale), afterwards the current decays exponentially until (e), where current was put through a wire wrapped around the superconductor. This drives the superconductor normal. A very rapid $\frac{dI}{dt}$ gives us an out-of-scale voltage and in (f) $\frac{dI}{dt} = 0$. The current decayed completely to zero. May we suggest the reader compares this with the graphs at the end of Chapter 2 (Figure 4b) keeping in mind that in

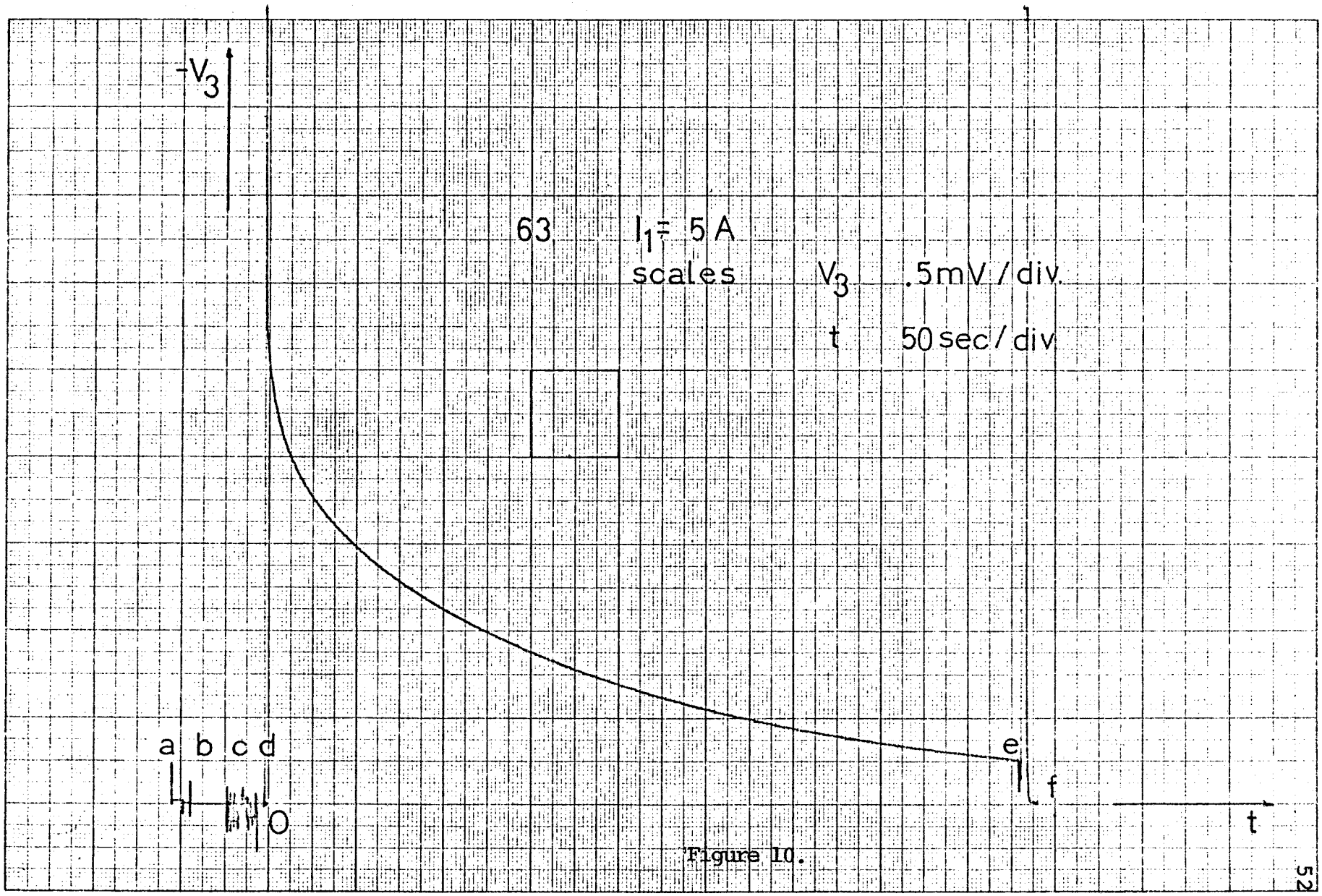

Figure 10.

Chapter 2 the time t_o was grossly exagerated compared to t.

The heater was put off. The current through the outer coils restored (at the same or a different value). The heater is activated again to damp out the current induced; the procedure can be started over again.

The way the joint was made was by cleaning the surfaces with a nylon sponge, fluxing and tinning them separately. We then pressed them together and heated them. A regular soldering iron was used. Solder was of the 50/50 type. The contact area was $3.6xm^2$. Microscopic inspection of the joint afterwards revealed some air bubbles, and an uneven thickness of the solder layer (between 40μm and 10μm). We refer to the pictures 5,6,7,8. Picture 5 shows a cross section of the soldered joint under a 40x magnification. So does Picture 6. The darker areas are the filaments of NbTi. One can see an airbubble at the joint surface in Picture 6. Picture 7 shows the solder near the air bubble under a 200x magnification. The thickness of the solderlayer is smaller at some places (Picture 8, same magnification 200x). The measured resistance were in the range $1.5x10^{-9}\Omega$ to $2.6x10^{-10}\Omega$ so that we had time constants from 120 to 750 sec. The induced current was not measured. At those time constants the drift of

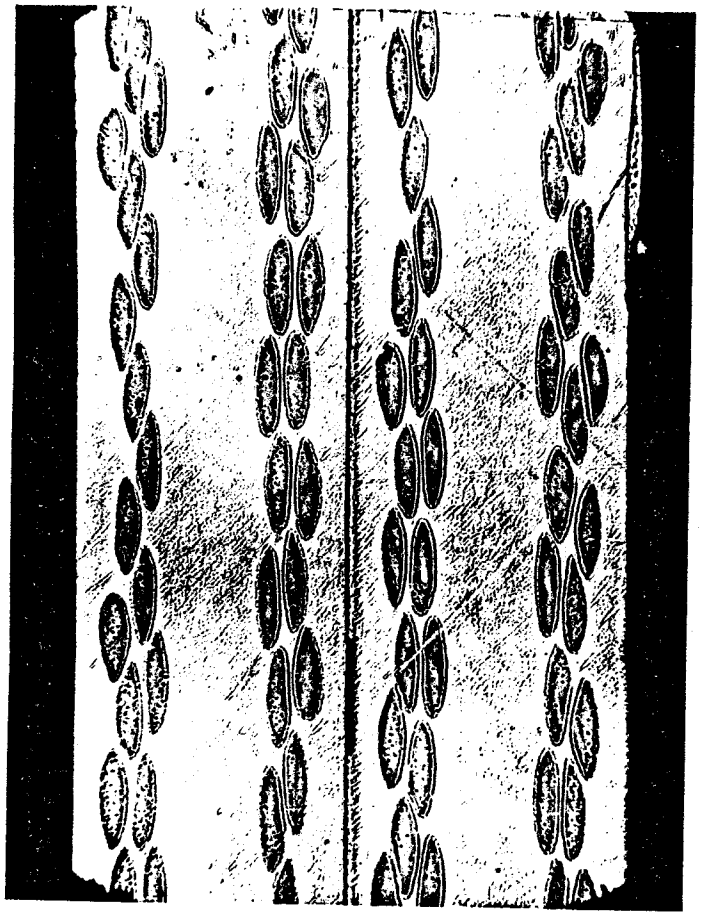

Picture 6. Soldered Joint, cross Section (40X)

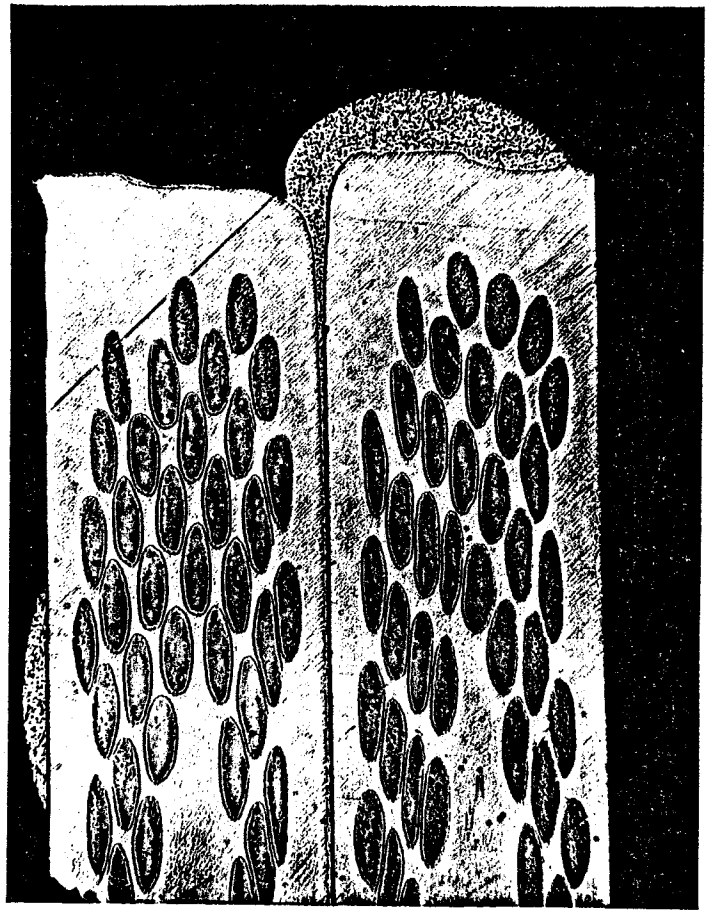

Picture 5. Soldered Joint, cross Section (40X)

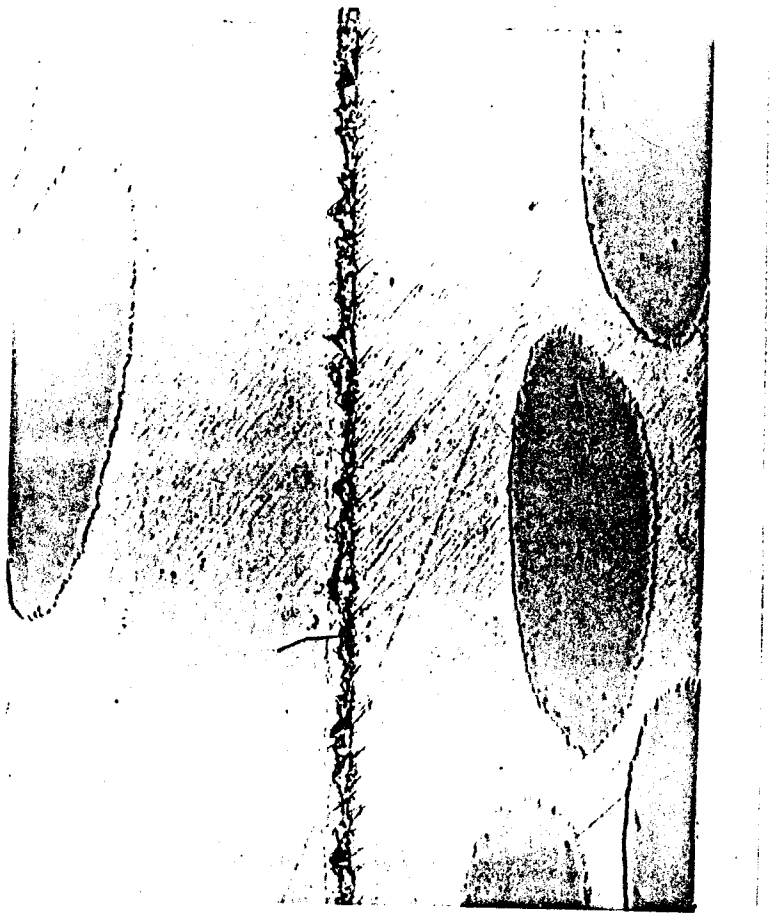

Picture 8. Detail of the Solder, thickness 10 µm (200X)

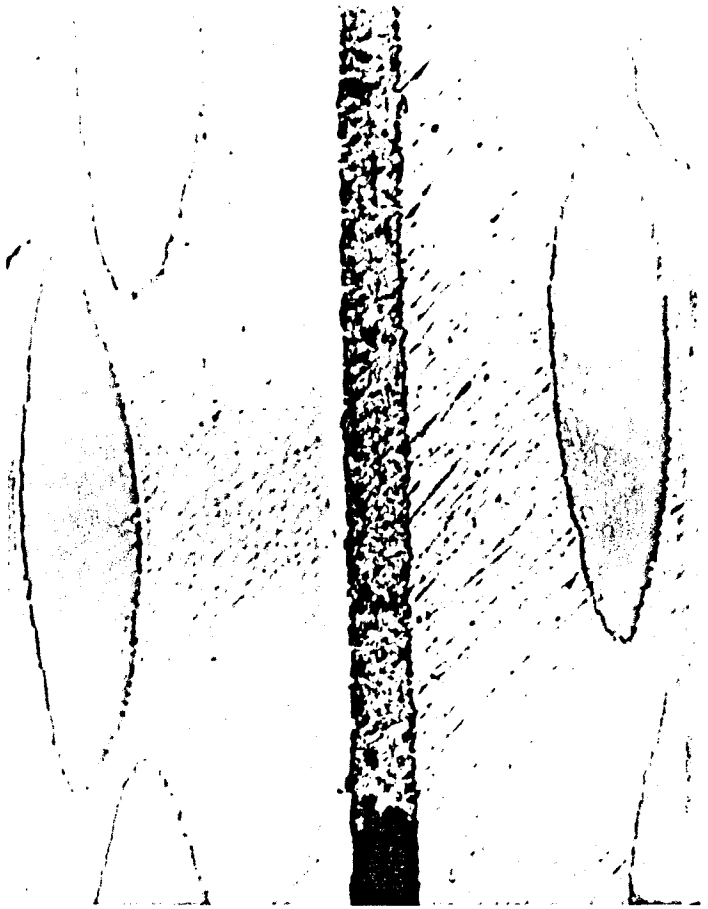

Picture 7. Detail of the Solder, thickness 40 µm (200X)

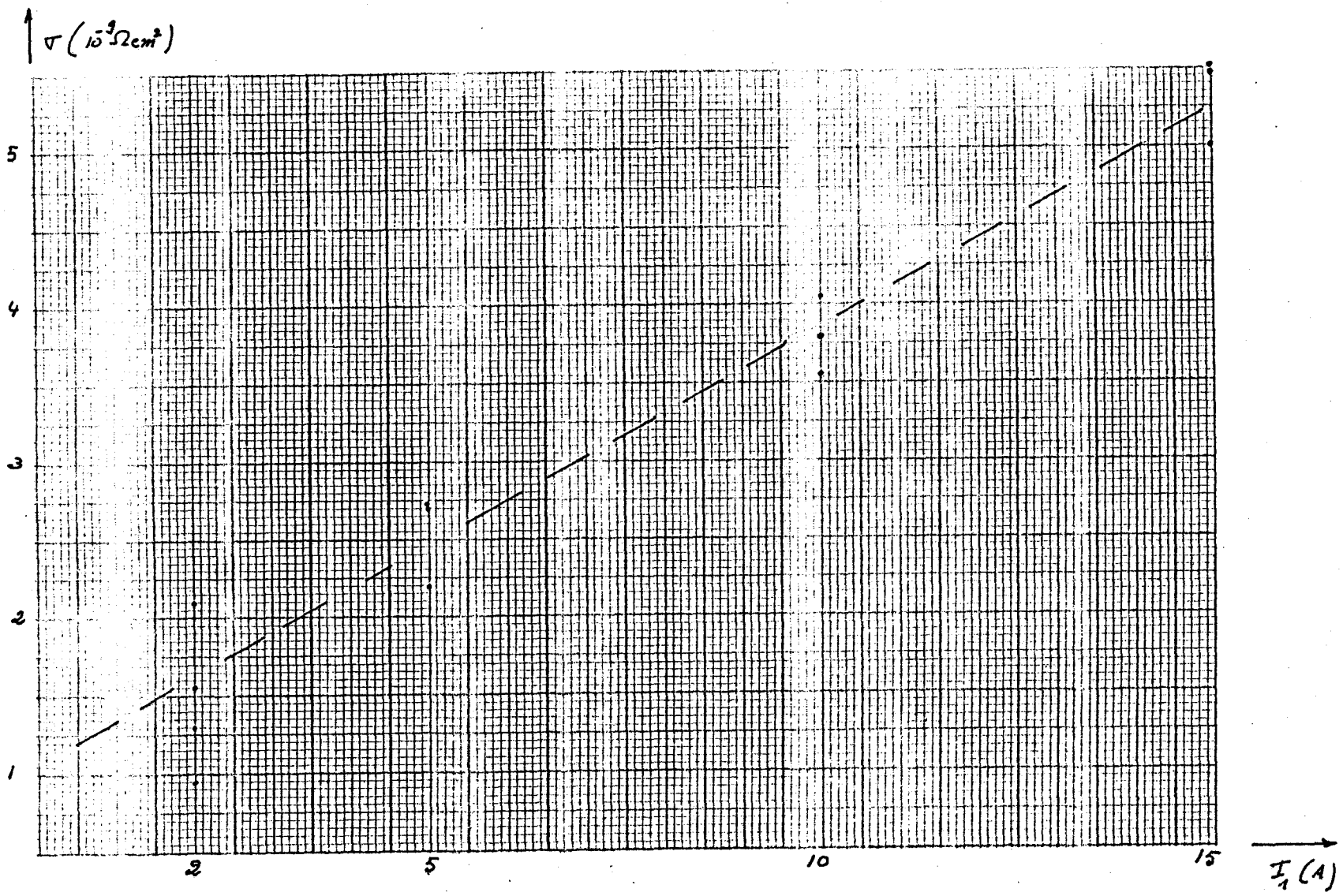

Figure 11. Soldered Joint #1, surface resistance.

$\frac{I_2}{I_1} \simeq 200$

$S = 3.5\ cm^2$

the integrator would become a problem. Figure 11 summarizes the results.

4.2 Silver Plated Joint

A first sample (#2) was made in the following way. The copper surface was first rubbed with a nylon sponge until it was shiny. It was then put for 10 min. in a mixture of nitric and sulfuric acid (brite dip #2); it was rinsed with water and dried with acetone. A silver electrode was used to electroplate it. The electrode was covered with cloth, and this cloth was moistened with an electrolyt. The plating was done by rubbing the electrode several times gently over the surface that would provide the joint. The sample was rinsed and dried with a piece of cotton wool. The joint was clamped between the stainless steel plates, three shims of 0.016" each were used to diminish the depth of the grooves. One compression washer was used for each of the two bolts. The voltage was measured and time constants in the range 375 sec to 401 sec obtained for resistances of $5.3 \times 10^{-10}\Omega$ to $5.0 \times 10^{-10}\Omega$. The contact area was measured when the sample was taken out. The contact area can easily be distinguished from the rest by its shiny look. We measured $1.4 cm^2$. In this case the joint stuck together but could easily be loosened with a screwdriver. Figure 12 summarizes the results for the

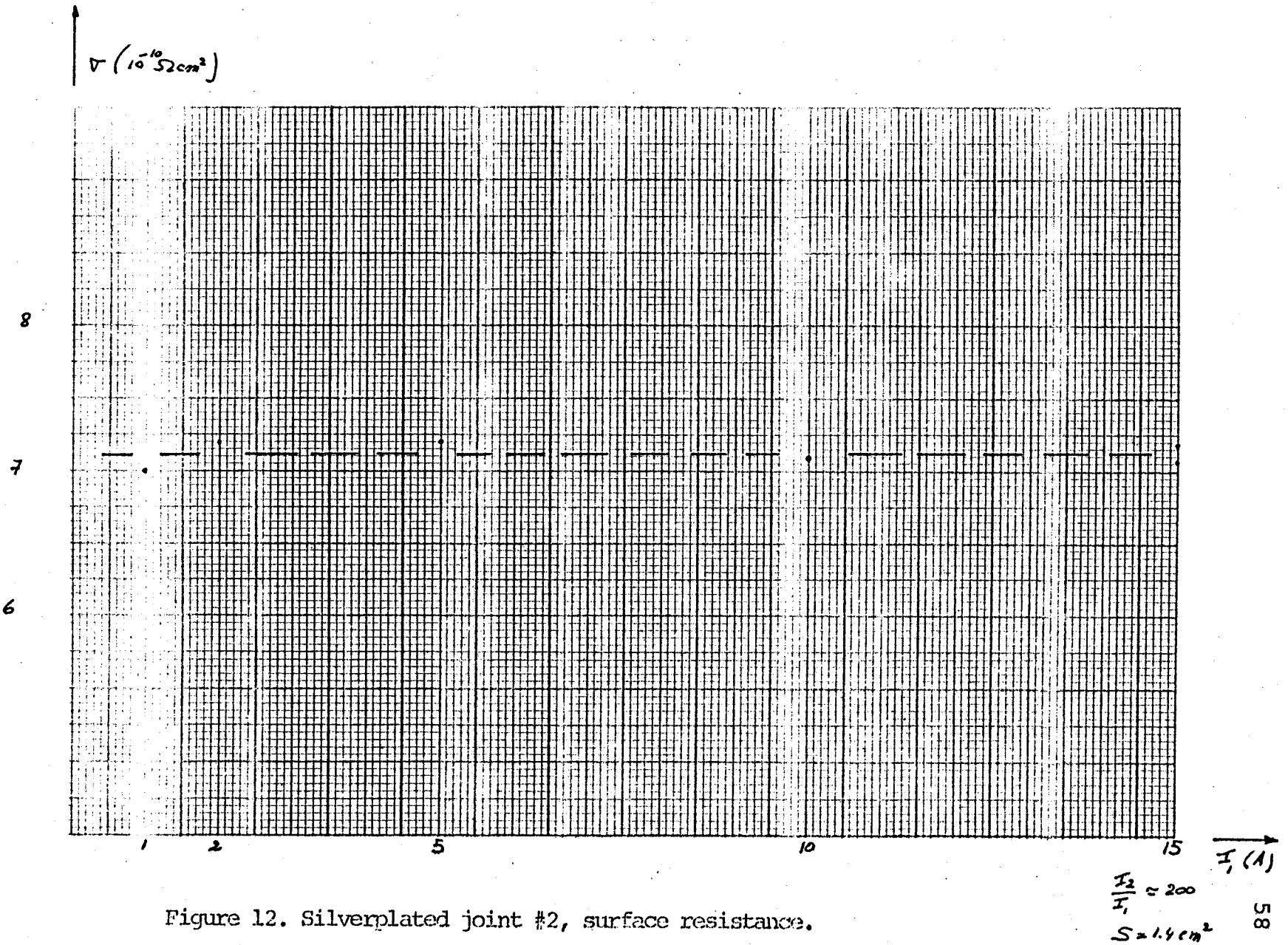

Figure 12. Silverplated joint #2, surface resistance.

surface resistivity.

The same sample was left in the open air for one day, rebolted and new measurements were made (#3). Higher resistances were obtained. Figure 13 summarizes the results.

In order to check the reproducibility of the results, a new silver plated sample was made. In making the joint the same procedure was used except that the sample was silverplated in an electrolitic bath. The thickness of the plating was smaller. The thickness was actually so small that the color of the copper underneath the silver gave a slight tint to the plated surface. More will be said later about the difference in plating method. The voltage was amplified and recorded.

This time measurements were also made were the voltage was integrated and recorded. A regular operational amplifier with a capacitor in the feed-back loop was used as integrator. Figure 14 is a typical recording of an integrated voltage (although it is from another sample). We again suggest the reader to compare this with the sketches at the end of the second chapter, (Figure 4d). In (a) the drift of the amplifier was adjusted if needed. The current in the external coils is interrupted in 0 giving a sudden drop (b). The current in the loop decays exponentially until (c) where the heater was put on. This drives

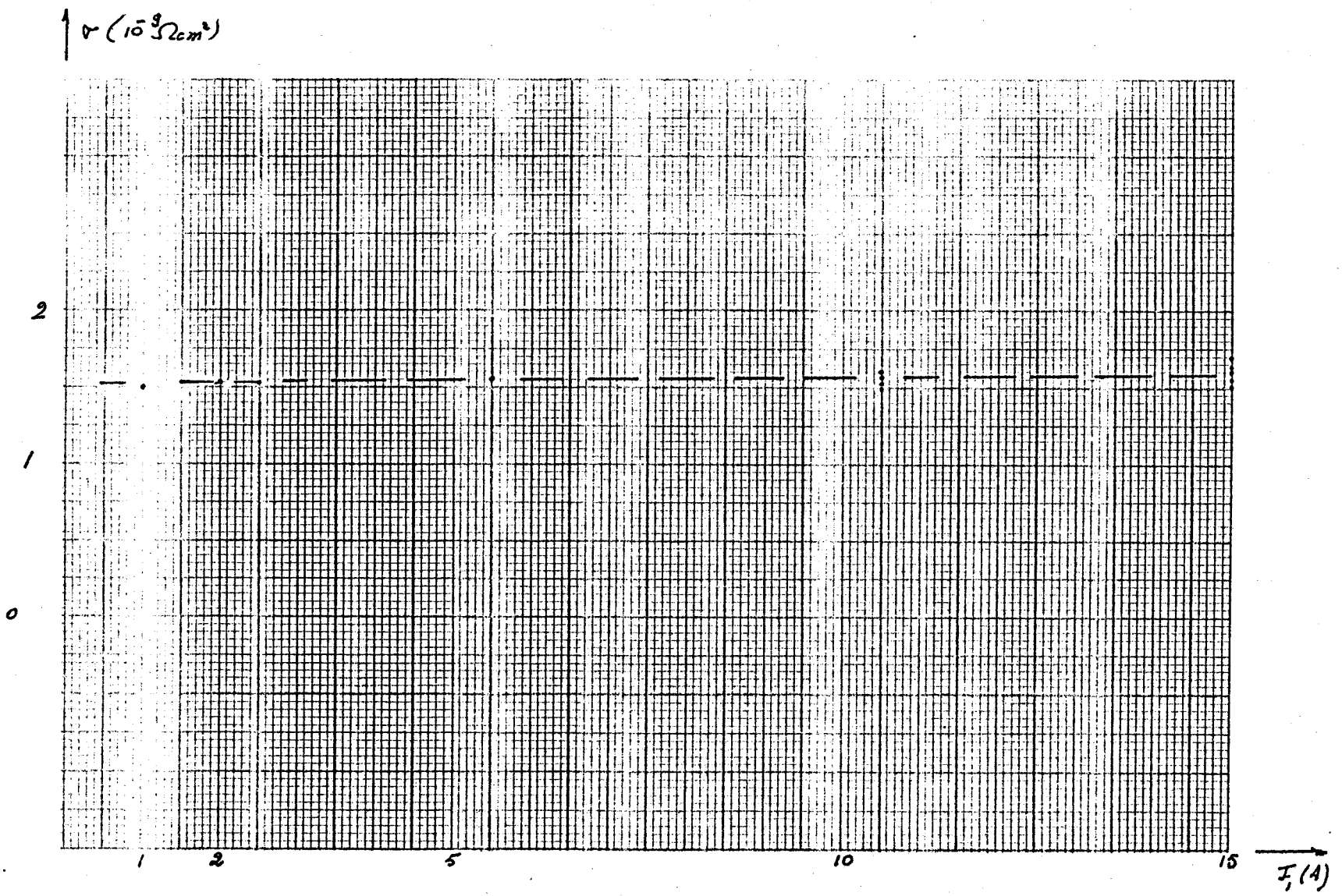

Figure 13. Silverplated Joint #3, surface resistance.

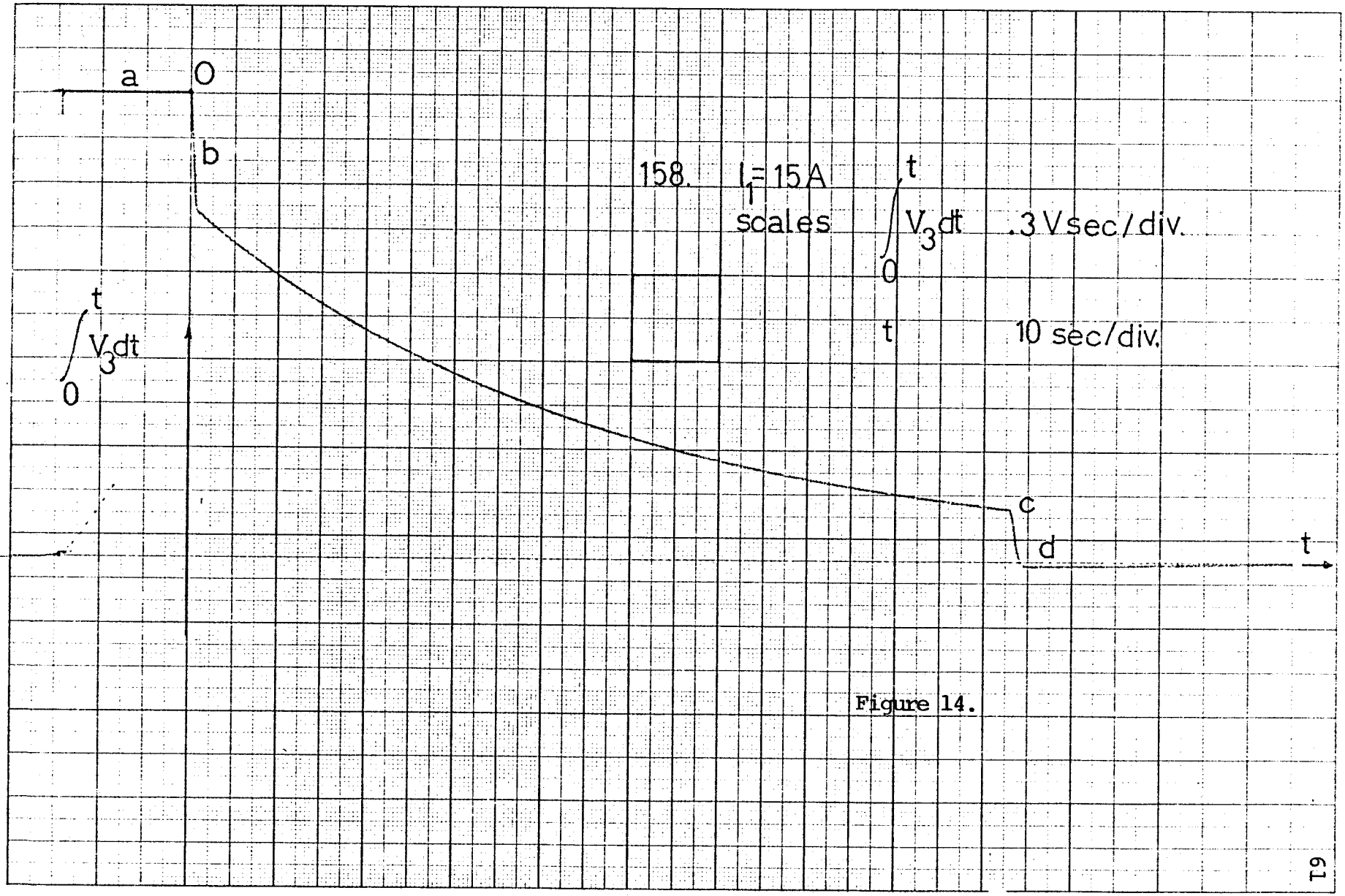
a
O
b
158.
I_1 = 15 A
scales
$\int_0^t V_3 dt$
.3 V sec/div.
t
10 sec/div.
$\int_0^t V_3 dt$
0
c
d
t

Figure 14.

the superconductor normal and the current goes rapidly to zero. We continue to record the integrated voltage at the end in order to check again the drift of the amplifier. $I_2(t_o)$ can be calculted easily from the integrated voltage. Remember that:

$$I_2(t_o) = \frac{1}{M_{23}} \left[- \int_{t_o}^{\infty} V_3 dt \right]$$

$$= \frac{1}{M_{23}} \left[\int_{o}^{t_o} V_3 dt - \int_{o}^{\infty} V_3 dt \right]$$

We can plot $I_2(t_o)$ as a function of I_1. The relation should be linear as long as the current carrying capacity of the joint is not exceeded. We can also compare this to

$$I_2(t_o) = \frac{M_{12}}{L_2} I_1(0)$$

where we had $M_{12} = 4.0 \times 10^{-5} H \ (\pm 0.5 \times 10^{-5})$

$$L_2 = 2.0 \times 10^{-7} H \ (\pm 0.1 \times 10^{-7})$$

so that $\frac{M_{12}}{L_2} = 200 \pm 35$. From Figure 5 we obtain $I_2 = 145\ I_1$. If we take into account the uncertainty on M_{23}, which comes through in the calculation of I_2 we obtain $I_2 = (145 \pm 12)\ I_1$. There is a difference which does not fall within the uncertainties of the measurements. This difference can be due to several factors. M_{12} too high, L_2

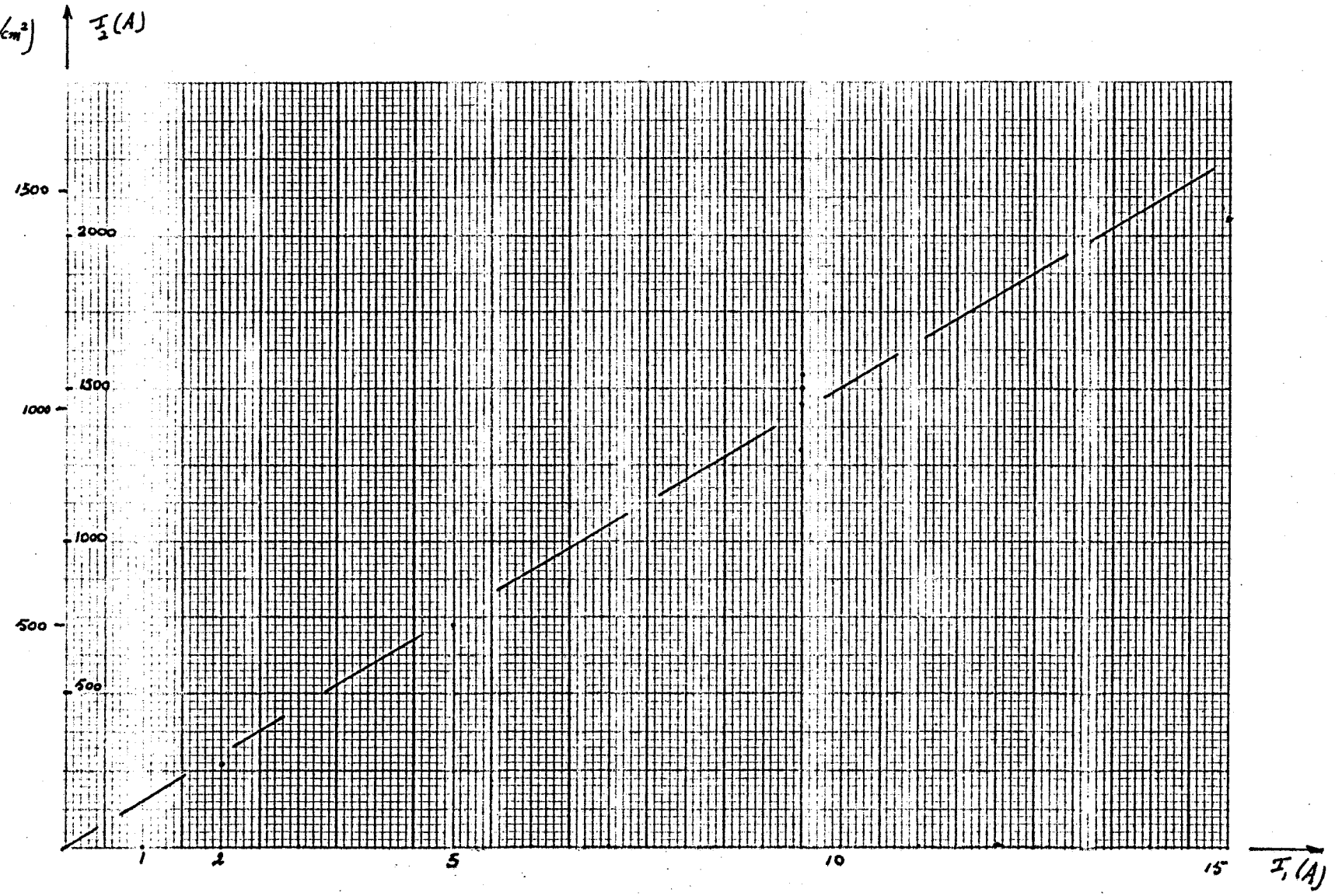

Figure 15. Siverplated joint #4, induced current vs. inducing current.

too low, M_{23} too high. Remember that M_{12} as well as M_{13} depends on the location of the sample holder in the magnetic field, while M_{23} only depends on the fixed geometry of the sample holder. From the integrated voltage M_{13} can be calculated using $M_{13} = \frac{1}{I_1} \int_0^\infty V_3 dt$. Lower values (0.12 - 0.13H) than the previous measurements (0.15H) might mean that the location of the sample holder was not exactly the sameas when the inductances were calibrated. This would also mean a lower M_{12} which could account for the difference. If we assume (worst case) that the total difference is due to an L_2 which would be larger in the superconductive state than what we measured in the normal state then it would mean that $L_2 = 2.75 \times 10^{-7}$H rather than the measured $L_2 = 2 \times 10^{-7}$H. The impact on this for the resistance calculating would be an increase of 37.5%. The surface resistivity are summarized on Figure 16.

4.3 Copper Joint

We also investigated a regular copper to copper joint in order to check whether a copper to copper contact could achieve the same low resistance as the silverplated contact. The surface was prepared in the following way.

TECHNOLOGY STORE, H. C. S. 66 MASS. AVE., CAMBRIDGE, MASS.

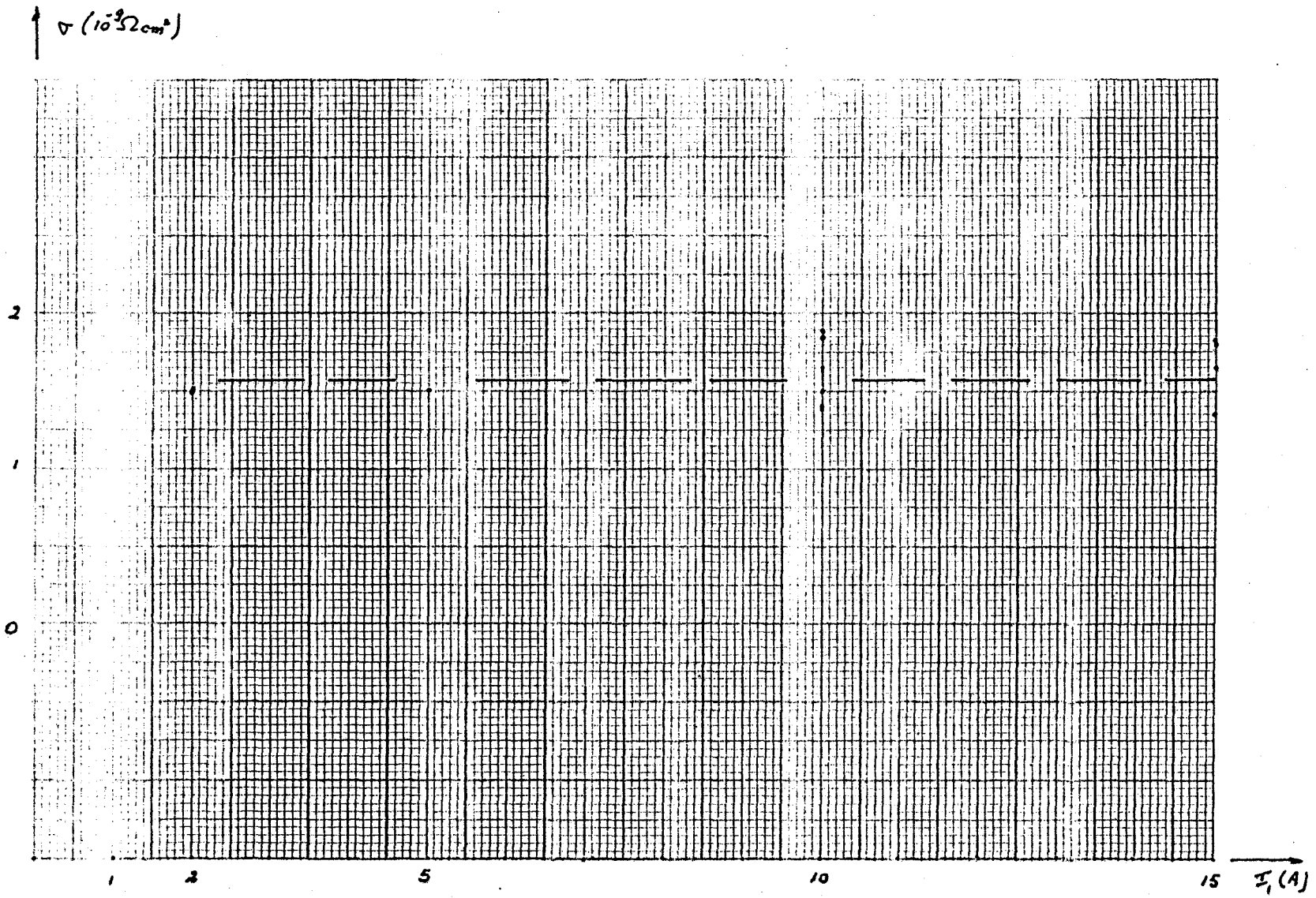

Figure 16. Silverplated joint #4, surface resistance.

- cleaned with a nylon sponge,
- cleaned with acetone to remove any oil staining.
- put in brite dip #2 for 20 min.
- cleaned with nylon sponge and water,
- dried with aceton,
- it was then put in a tank with boiling freon. The vapors condensed on the surface and removed the thin residue acetone leaves.

Four 0.016" shims were used and the joint clamped together with one washer for each bolt. Figure 18 gives the results for the surface resistance. The area was $1.43 cm^2$. The calculated I_2 as a function and I_1 appears on Figure 17. We obtain $I_2 = 145\ I_1$ which agrees with what we found for the silverplated joint.

The sample was left overnight in the Dewar with the two surfaces still in contact. We were led to the conclusion that oxygen had condensed in the Dewar and formed CuO_2 on the contact surfaces on the basis of two observations:

i) the sample holder was stuck in the Dewar,

ii) when this problem was solved and the measurements resumed, much higher resistances were obtained.

TECHNOLOGY STORE, H. C. S. ... AVE., CAMBRIDGE, MASS.

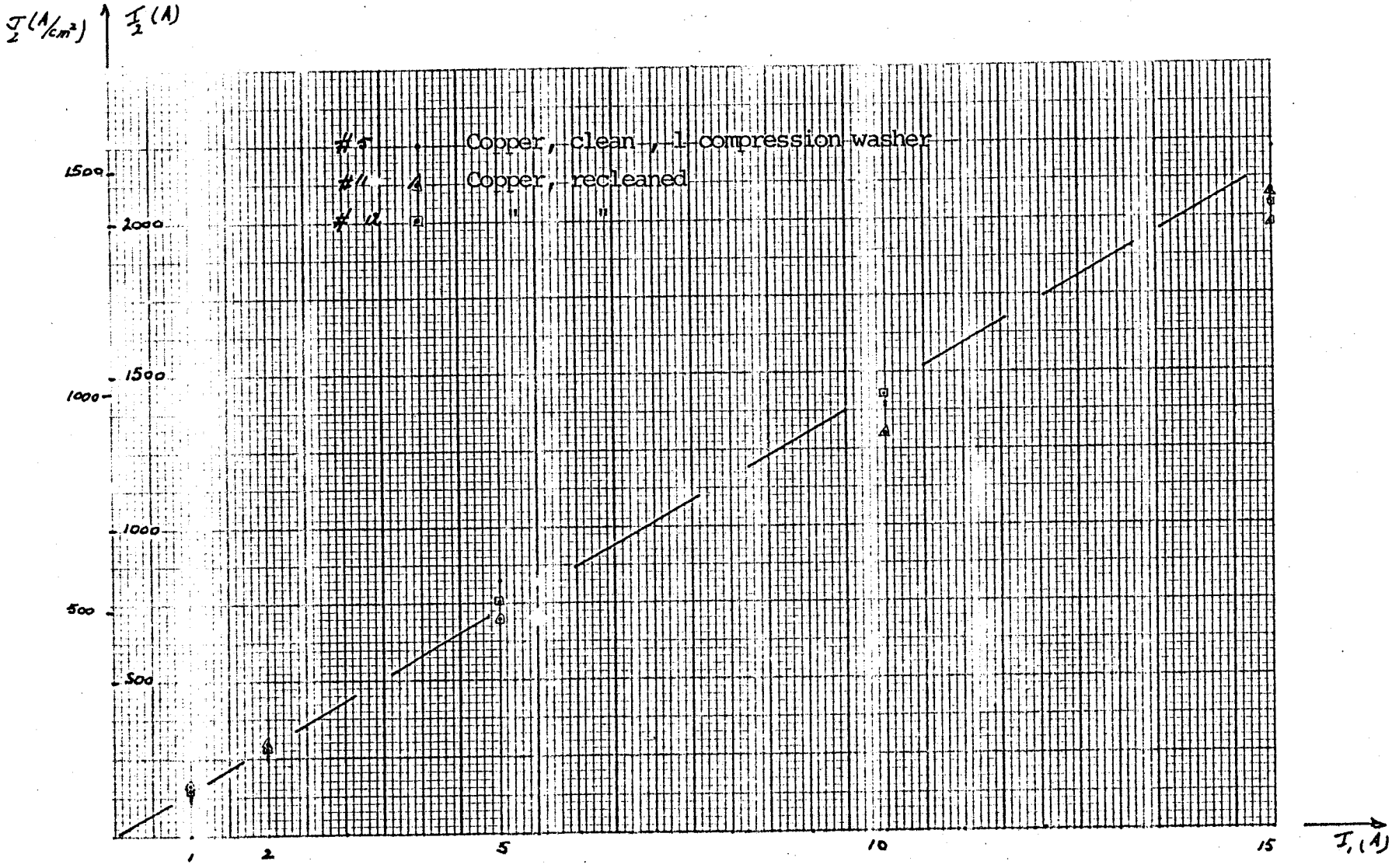

Figure 17. Clean Copper Joint, Induced Current vs. Inducing Current.

TECHNOLOGY STORE, M. C. S. 40 MASS. AVE., CAMBRIDGE, MASS.

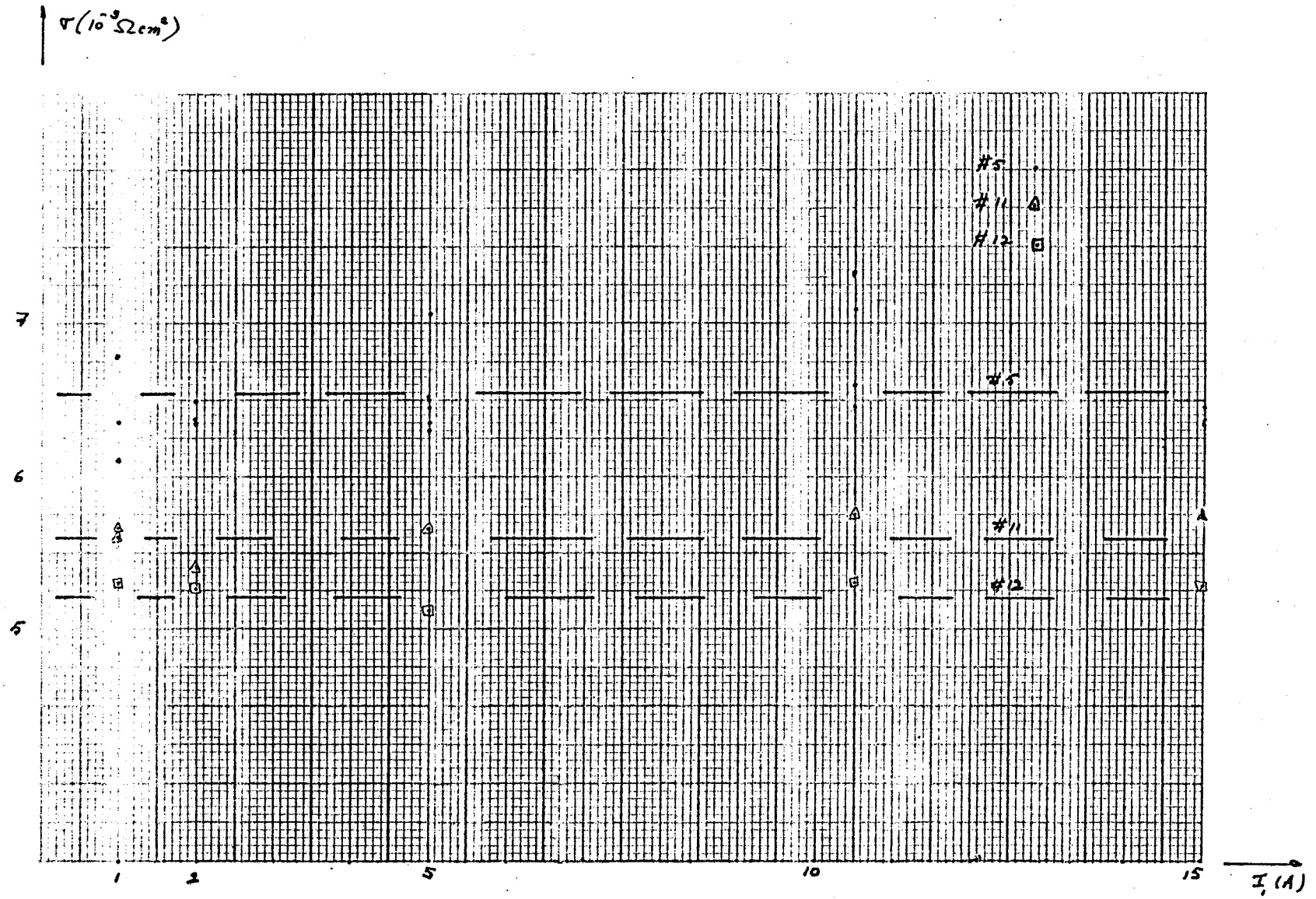

Figure 18. Clean copper joint, Surface Resistance.

Measurements were made with 2 compression washers (#6), 1 compression washer (#7), 2 compression washers again to see if the bolting and unbolting had any effect on the measurements (#8) and 3 compression washers (#9). The sample was left overnight in helium and some measurements were done again (#10) yielding the same results. The results are summarized in Figure 19 and Figure 20.

In order to see whether the data for a clean surface could be reproduced, new measurements were made. The surface was again rubbed with the nylon sponge, put in brite dip for 15 sec, rinsed with water, dried with acetone and cleaned with freon vapor. The data are summarized on Figure 17 and Figure 18 for comparison (#11). To see whether unbolting and rebolting the sample had any influence on the measurements, new measurements were made after the sample had been taken out, unbolted, rebolted, and put back again (#12). Figures 17, 18.

Measurements were also made for a sample where a piece of copper (38/1000 thick) was inserted between the two surfaces to be jointed. We obtained $R \simeq 1.5 \times 10^{-8} \Omega$. It was not possible to relate this quantitatively to the previous measurements because when we unbolted the sample it was noticed that when the joint was made the copper piece had moved slightly so that the geometry was too complicated to make calculations. Compared with the normal joint, we

TECHNOLOGY STORE, M. C. S. 40 MASS. AVE., CAMBRIDGE, MASS.

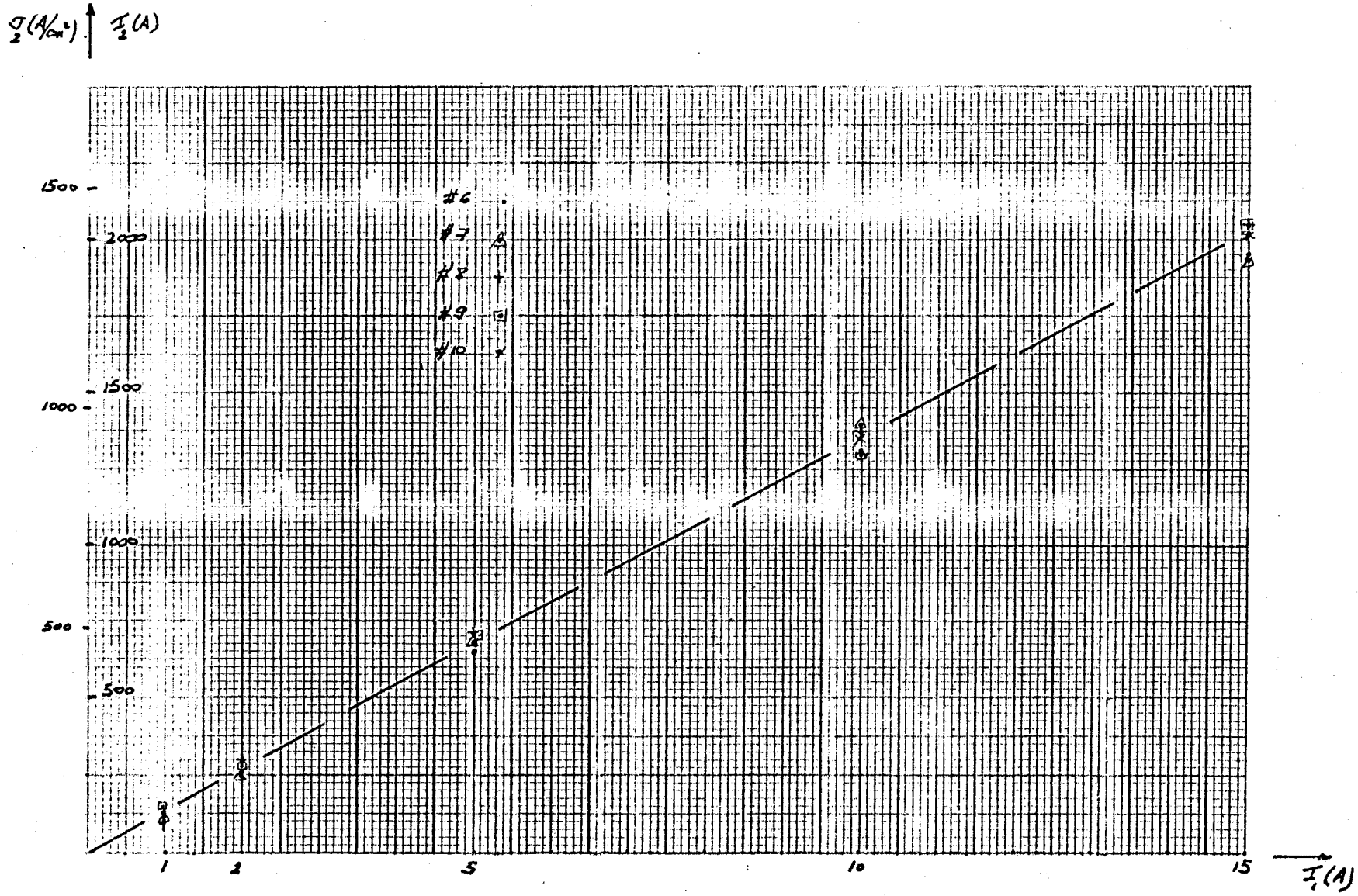

Figure 19. Oxidised Copper Joint, Induced Current vs. Inducing Current.

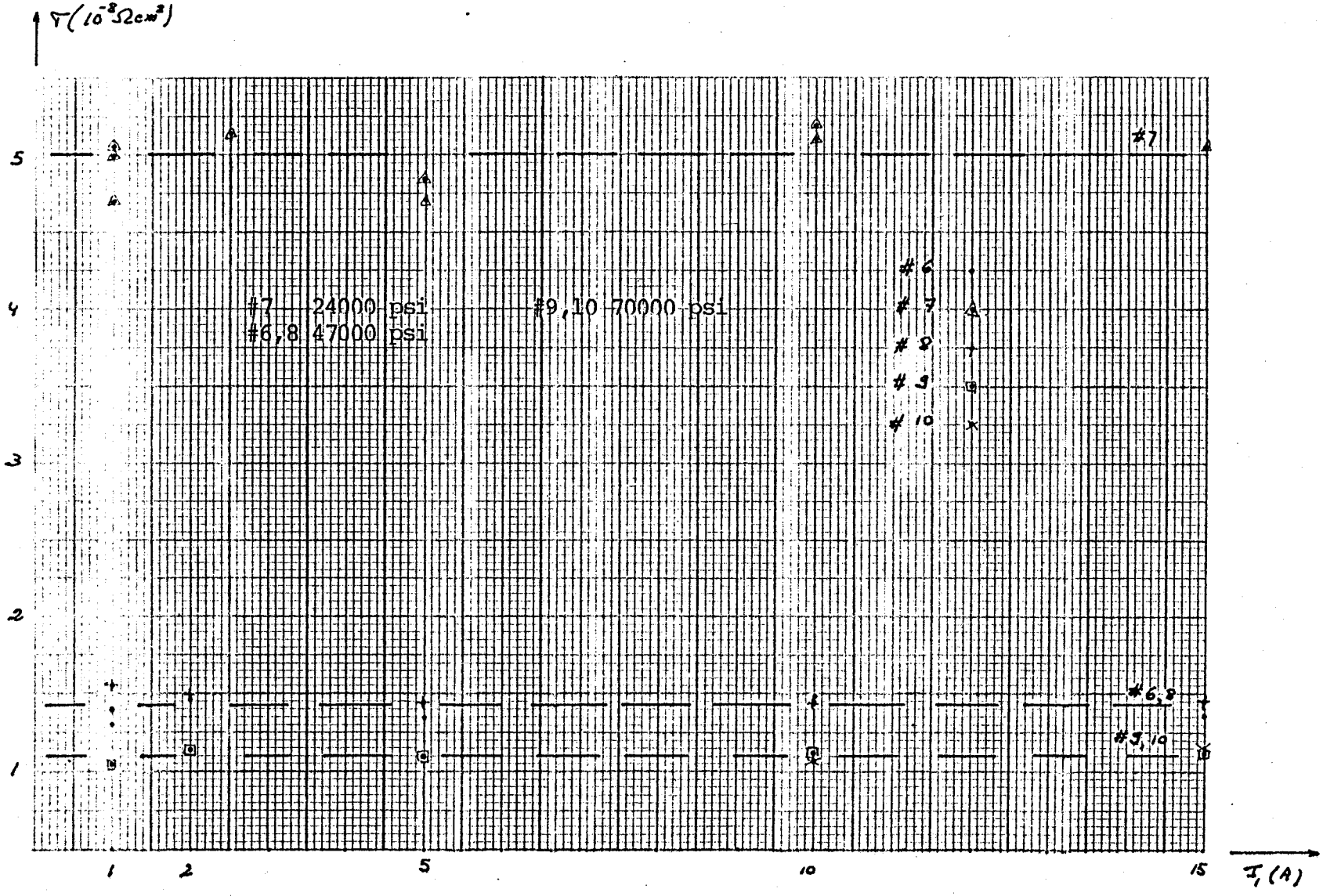

Figure 20. Oxidised Copper Joint, Surface Resistance.

have two additional resistances. First one more contact resistance, second the resistance in the additional copper piece. The results are compatible with the assumption that for a normal joint the resistance is due for the major part to the contact resistance.

4.4 Summary of the Results

We give briefly an overview of the different samples.

#1 Soldered (50/50 solder).

#2 Silverplated.
The surface was first cleaned with a nylon sponge, put in brite dip, rinsed with water and dried with acetone. Silverplated by hand, rinsed and dried. This sample was so clean that when we unbolted the joint it was still sticking together.

#3 Same sample, allowed to oxidize in the air for 1 day.

#4 Silverplated, same procedure as for sample #2 except that the silverplating was done in an electrolytic bath.

#5 Clean copper to copper surfaces.
Cleaned with a nylon sponge, brite dip, water and aceton, freon vapors were used to remove the film left by the acetone.

TECHNOLOGY STORE, H. C. S. 40 MASS. AVE., CAMBRIDGE, MASS.

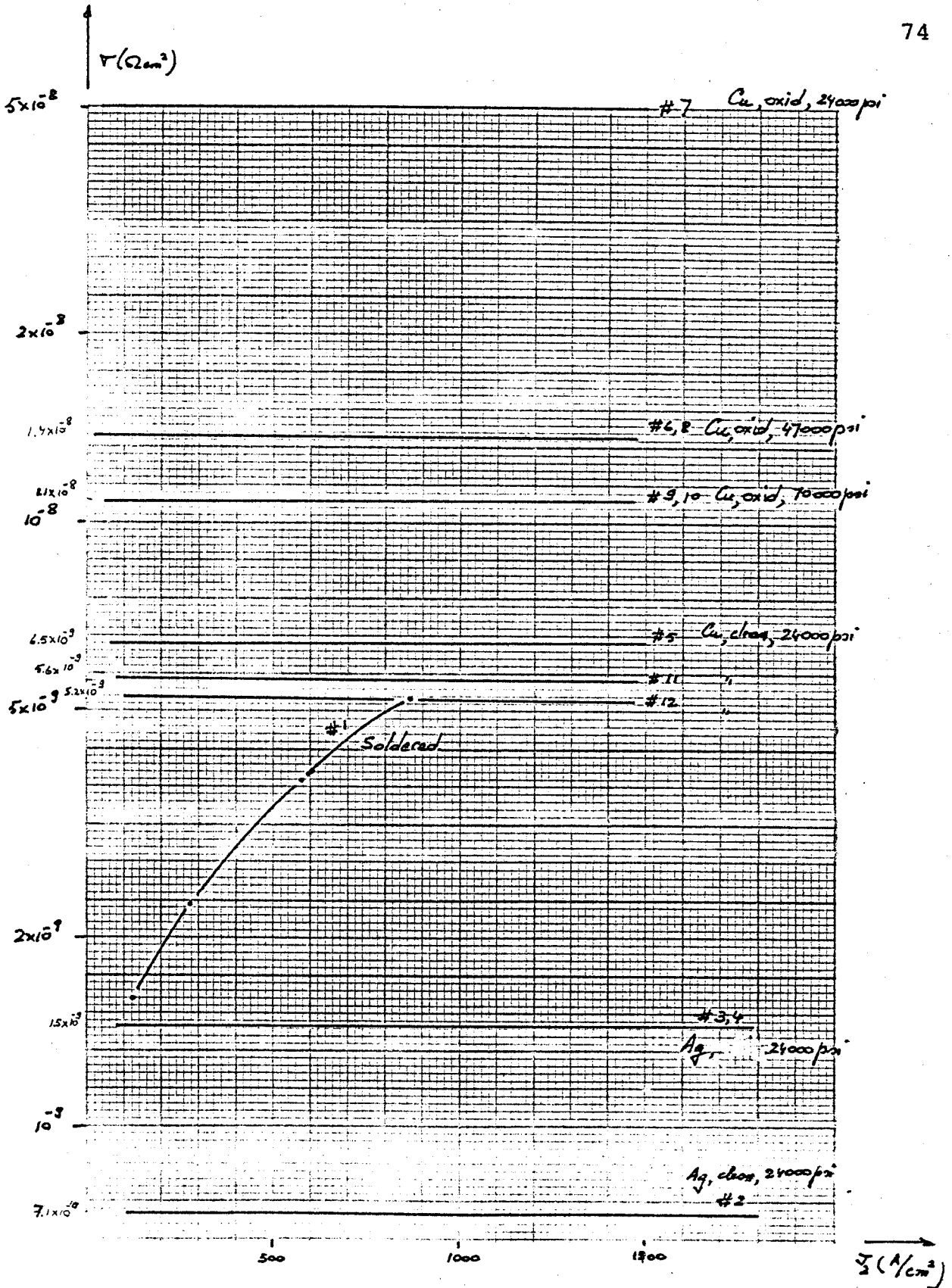

Figure 21.

TABLE 2. SUMMARY OF RESULTS

Joint Number	Surface Condition	Area of the Joint sq.i	Area of the Joint cm^2	Time Constant sec	Resistance Ω	Current Density A/cm^2*	Pressure psi	Pressure $10^5 N/m^2$	Contact Resistance Ωcm^2
#1	Soldered joint	0.54	3.5	130	1.5×10^{-9}	850+	--	--	5.2×10^{-9}±
#2	Silver plated	0.22	1.4	390	5.1×10^{-10}	2000+	24000	1700	7.1×10^{-10}
#3	Silver plated oxidized	0.22	1.4	180	1.1×10^{-9}	2000+	24000	1700	1.5×10^{-9}
#4	Silver plated	0.23	1.5	200	1.0×10^{-9}	1500	24000	1700	1.5×10^{-9}
#5	Copper freshly cleaned	0.22	1.4	45	4.5×10^{-9}	1500	24000	1700	6.5×10^{-9}
#6	Copper oxidized	0.22	1.4	20.4	9.8×10^{-8}	1500	47000	3400	1.4x-0^{-8}
#7	Copper oxidized	0.22	1.4	5.6	3.6×10^{-8}	1500	24000	1700	5.0×10^{-8}
#8	Copper oxidized	0.22	1.4	19.4	1.0×10^{-8}	1500	47000	3400	1.4×10^{-8}
#9	Copper oxidized	0.22	1.4	25.4	7.9×10^{-9}	1500	70000	5000	1.1×10^{-8}
#10	Copper oxidized	0.22	1.4	25.1	8.0×10^{-9}	1500	70000	5000	1.1×10^{-8}

(continued)

Table 2 (continued)

#11	Copper freshly cleaned	0.22	1.4	50	4.0×10^{-9}	1500	24000	1700	5.6×10^{-9}
#12	Copper clean	0.22	1.4	55	3.7×10^{-9}	1500	24000	1700	5.2×10^{-9}
#13	Copper sandwich	2x0.15	2x1	13	1.5×10^{-9}		24000	1700	---

$^{+}$Nd measured. Estimated from $I = \frac{M_{12}}{L_2} I_1$

*This is not a maximum current density but the maximum current density at which the measurements were made.

$^{\mp}$Dependent on current

CHAPTER 4

DISCUSSION OF THE RESULTS AND CONCLUSION

1. Discussion

1.1 Soldered Joint

As reported previously an extensive library search did not provide much data. Data for soldered joints are reported in (9), (17).

Both used the volt-ammeter method. In the report[9] recorder traces of voltage in function of current are reproduced. The voltage tracesare erratic and a relatively wide spread in data for current sweeps at identical conditions are reported. A special modificatin of the sample (saw-cut) to give a higher joint resistance and an easier to measure voltage drop did not yield the desired results. All this is in sharp opposition with our experiment. In our case the data could be easily measured, once the experiment was set up and we would tend to conclude that it is worthwhile to use this more elaborate method for future measurements of the resistivity of soldered joints.

Let us compare the results. Reference (9) obtained that for 50/50 solder at zero field the surface resistivity is of the order of $1x10^{-8}$ to $2x10^{-8}\Omega cm^2$. They have a solder thickness[b] of 100μm and a copper path length (a) of two times 150μm. At 16kG and 4.2k they calculate the

joint surface resistivity with

ρ_{cu} (copper bulk resistivity OHFC, R/R = 150) $1.7\times10^{-7}\Omega cm$

ρ_{so} (solder bulk resistivity 50/50 solder) $2.2\times10^{-6}\Omega cm$

$$\rho_s = 2\rho_{cu}\, a + \rho_{so}\, b$$

$$= 2\times1.7\times10^{-8} \times 0.015 + 2.2\times10^{-6} \times 0.010$$

$$= .051 \times 10^{-8} + 2.20 \times 10^{-8}$$

$$= 2.251 \times 10^{-8}\Omega cm^2$$

Doing the same calculation, in our case with

$$a = 100\mu m = 0.01 \text{ cm}$$

$$b = \frac{40\mu m + 10\mu m}{2} = 25\mu m = 0.0025 \text{ cm}$$

(we take an average solder thickness)

$$\rho_s = 2 \times 1.7 \times 10^{-8} \times 0.01 + 2.2 \times 10^{-6} \times 0.0025$$

$$= 0.34 \times 10^{-9} + 5.5 \times 10^{-9}$$

$$= 5.8 \times 10^{9}\Omega cm^2$$

Although the 50/50 solder is superconducting at zero field and 4.2k, the surface resistivity of a soldered joint drops by a factor fo only 2 to 3 going from 8T to 0T (27). Our measured values $1\times10^{-9}\Omega cm^2$ to $5.5\times10^{-9}\Omega cm^2$ are consistent with this calculation. A new and interesting result is the dependence of the resistance on the induced current.

Reference (17) gives a surface resistivity of 1.06×10^{-8} Ωcm^2 for 50/50 solder of T = 4.2k, B = 7 Tesla. As the joint resistance component due to the solder is the most important part and no solder thickness was given it is difficult to compare this with our data. However, assuming that the same solder thickness was achieved and again taking into account the decrease of the surface resistivity with decreasing magnetic field, we conclude that our data agree with prevously published results.

1.2 Silverplated Joint

Let us summarize briefly the results from the literature

D. Hay (28) obtained a surface resistivity of $2 \times 10^{-10} \Omega cm^2$, for a current density of $1000 A/cm^2$ at a pressure of 3000 psi.

J. Zar (18) made measurements for three silver plated samples obtaining

	ρ_s at 1000 psi (Ωcm^2)	at 4000 psi (Ωcm^2)
#1	1.05×10^{-8}	8.8×10^{-9}
#2	1.2×10^{-7}	4.5×10^{-8}
#3	8.7×10^{-9}	7.0×10^{-9}

Leaving #1 untouched for three weeks yielded

#1 3.3×10^{-7} 5.9×10^{-8}

The decrease of the logarithm of the surface resistivity with pressure was linear for the clean samples and more rapid for the oxidized sample.

We obtained at 24000 psi

#2 $7.1 \times 10^{-10} \Omega cm^2$

#3 $1.5 \times 10^{-9} \Omega cm^2$

#4 $1.5 \times 10^{-9} \Omega cm^2$

The value of $1.5 \times 10^{-9} \Omega cm^2$ is consistent with a logarithmic extrapolation of the data Zar obtained in the range 1000 to 4000 psi. Additional measurements inthe intermediate pressure range would be necessary to support or unvalidate the assumption that the surface resistance for a clean silverplated conductor is of the order of $1.1 \times 10^{-8} \Omega cm^2 \times 10^{-0.035 \frac{p}{1000psi}}$. This yield $1.0 \times 10^{-8} \Omega cm^2$ at 1000 psi

$8.0 \times 10^{-9} \Omega cm^2$ at 4000 psi

$1.7 \times 10^{-9} \Omega cm^2$ at 24000 psi

Several S.E.M. pictures were made in order to further investigate the nature of the silverplating. Picture 9 shows an unpressed portion of the hand plated surface. The magnification is 5000 (the white bar below is 10μm long) and the surface is tilted at a 15° angle. Comparison of

this picture to picture 2 (copper surface) makes clear that the silverplating provides a rough regular surface. The roughness is slightly higher for the handplated surface (Picture 9) than for the surface that was plated in a both (Picture 11). This seems to hold also for the parts of the surface that were pressed (Picture 10, Picture 12). Notice the effect on the surface roughness of pressing the surfaces together (compare Picture 9 and 10 for the handplated sample and Picture 11 and 12 for the sample plated in a bath). Picture 13 shows the pressed surface of Sample 4 (bath plated) at a lower magnification. We want to point out the uneven distribution of the pressure.

Pictures were also made of cross sections in order to measure the thickness of the silverlayer (Picture 14, 15, magnification 20,000). However, no definite boundary between copper and silver could be designated. It seems that some alloying has taken place. Further investigations with microprobe are being done. One feature can be pointed out. The depth of the cracks is for the handplated sample (Picture 14) larger than for the other (Picture 15) which agrees with the higher original roughness. The high roughness of the handplated joint can be the reason its sticking together (sample #2) due to mechanical interlocking of the surfaces. A higher resulting contact area would then account for the lower resistance.

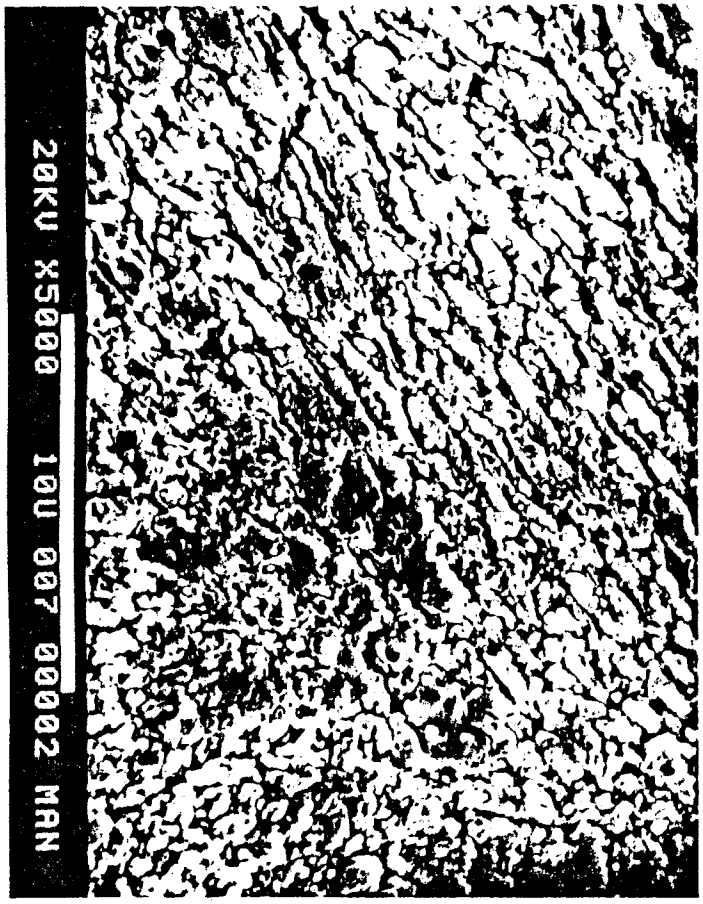

Picture 10. Silverplated surface, pressed, sample #2 (5000X)

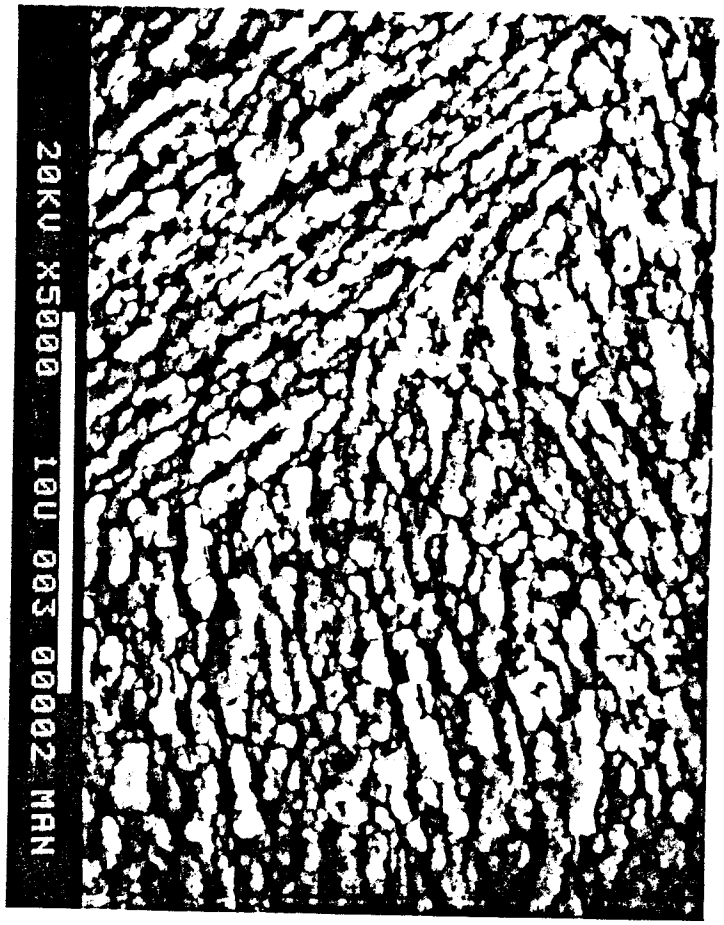

Picture 9. Silverplated surface, unpressed, sample #2 (5000X)

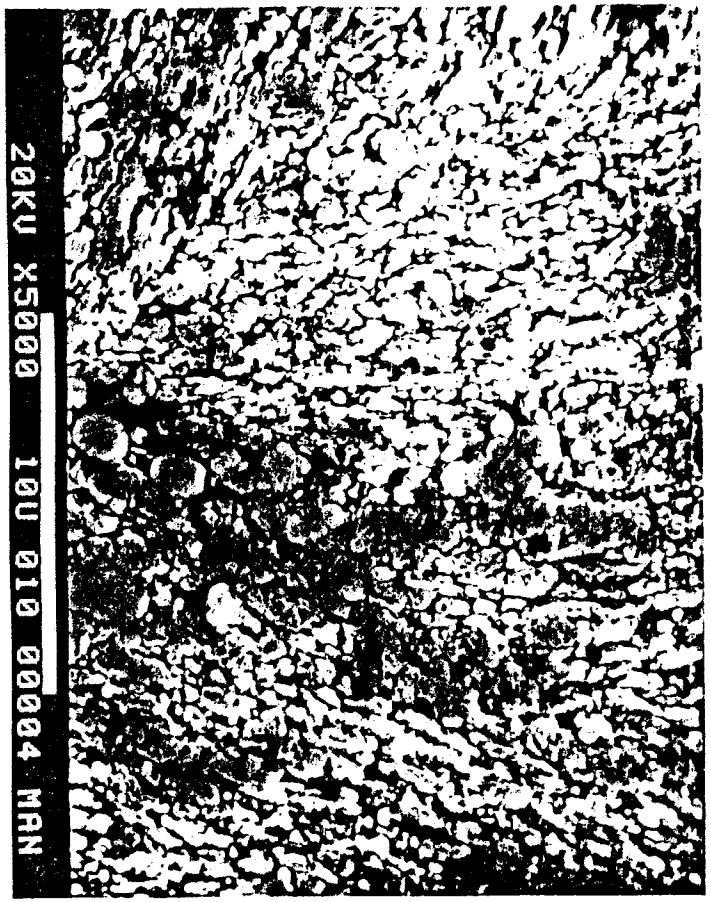

Picture 12. Silverplated surface, pressed, sample #4 (5000X)

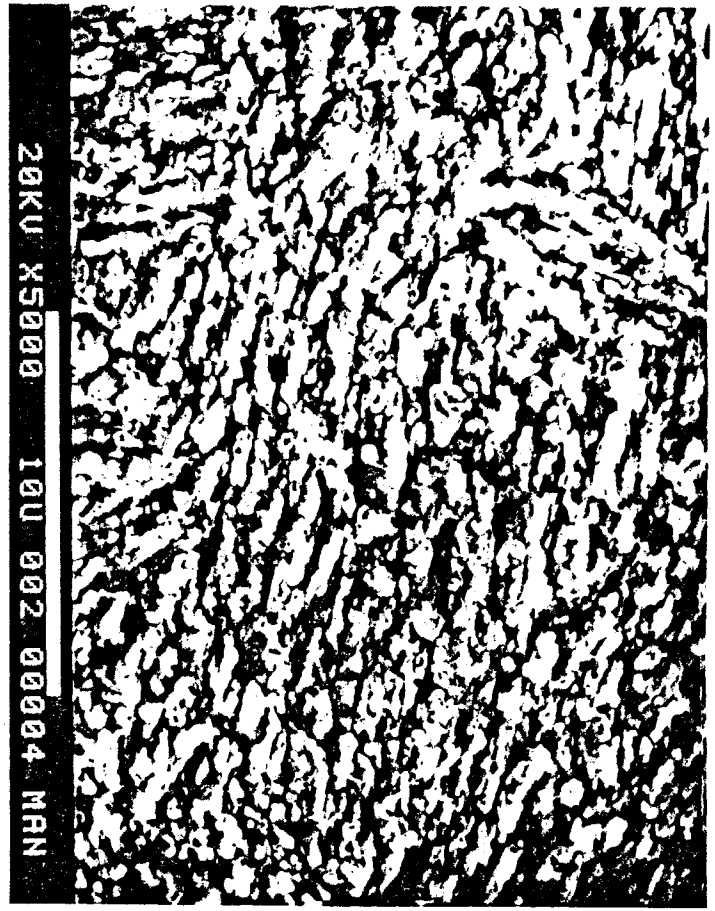

Picture 11. Silverplated surface, unpressed, sample #4 (5000x)

Picture 13. Silverplated surface, pressed, sample #4 (1000x)

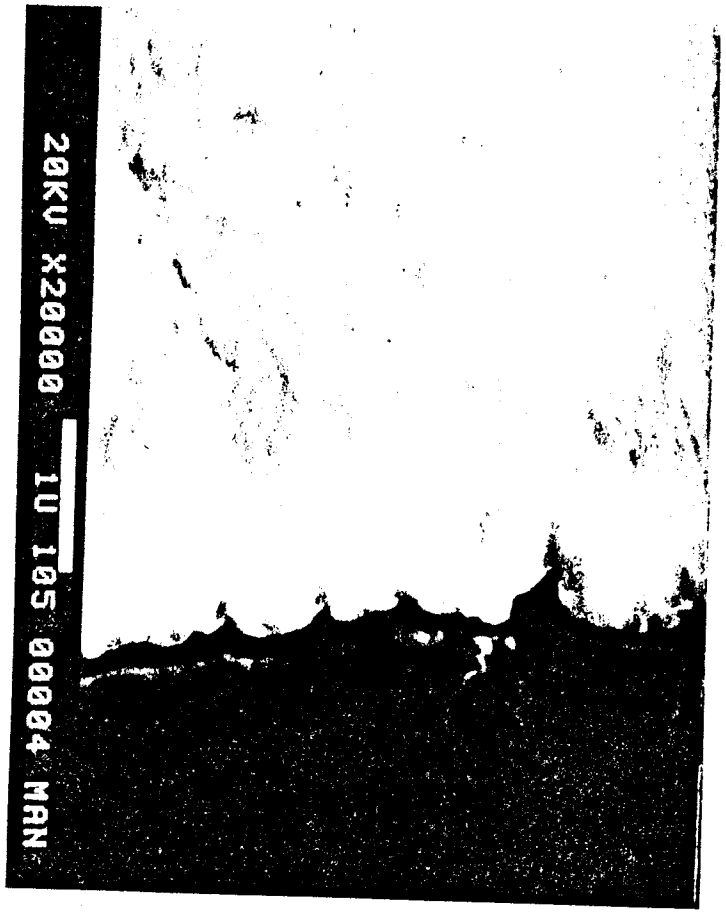

Picture 15. Cross section of the silver layer, pressed, sample #4, (20 000x)

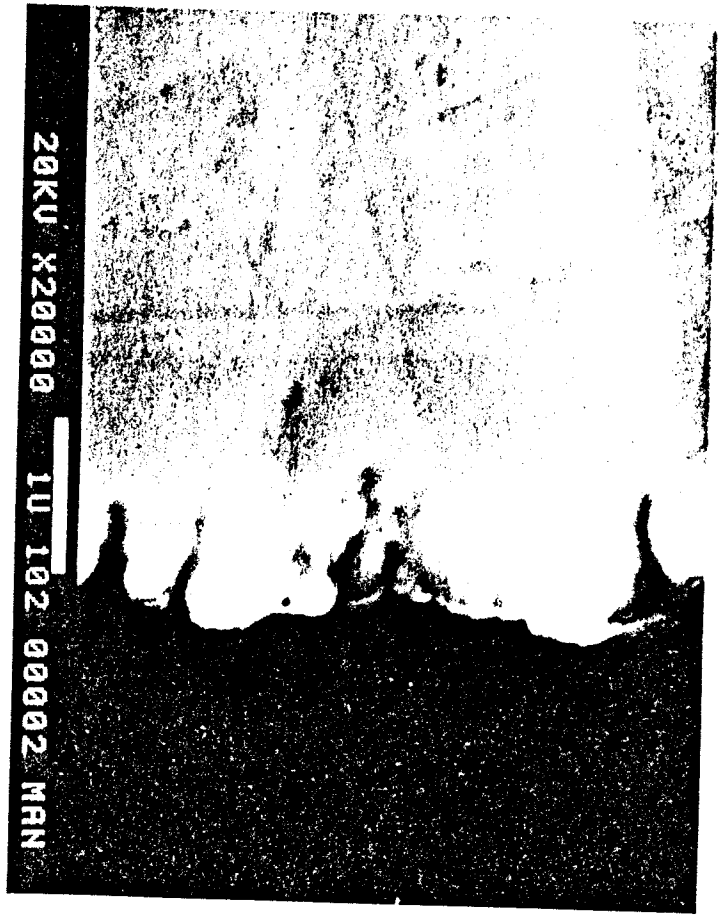

Picture 14. Cross section of the silver layer, pressed, sample #2, (20 000x)

1.3 Copper to Copper Contact

Zar (18) obtained the following results

	$\rho_s \Omega\text{-cm}^2$ at 1000 psi	$\rho_s \Omega\text{-cm}^2$ at 3000 psi
Copper, freshly cleaned	9.5×10^{-7}	6.3×10^{-7}
Copper, cleaned 2 months earlier	6.1×10^{-5}	2.7×10^{-5}

R. Holm and W. Meissner (29) in their very interesting article from 1932, in which they also prove that bare superconductor -- superconductor contacts have zero resistance, obtained the values $2.5 \times 10^{-9} \Omega cm^2$ at 57000 psi for very clean copper surfaces (they also observed the fact that the surfaces were sticking together), 1.2×10^{-8} Ωcm^2 at 57000 psi for a surface that did not stick together. Note that the values of the resistance are always at a pressure equal to the yield strength of the material. This is a consequence of their method, and the quoted results are always the surface resistivity between two surfaces of bulk material.

Our values are

	Ωcm^2 at 24000 psi	Ωcm^2 at 47000 psi	Ωcm^2 at 7000 psi
Copper fully cleaned	6.5×10^{-9} 5.6×10^{-9} 5.2×10^{-9}		
Copper oxidized (1 day)	5×10^{-8}	1.4×10^{-8}	1.1×10^{-8}

Our values seem to be significantly lower than those obtained by Zar and more in accordance with what R. Holm and W. Meissner obtained. It is, however, clear from our data and those of Zar that the oxide layer has an enormous influence on the surface resistance. Comparing the data points for sample 5, 11, 12 on Figure 18 also show that the scattering of the data points is reduced after the joint has been subjected to very high pressure.

1.4 Other Contact Materials

Zar (18) also reports results for materials we did not test.

	$\rho_s (\Omega\text{-cm}^2)$ at 1000 psi	$\rho_s (\Omega\text{-cm}^2)$ at 4000 psi
Tin on copper clean	2.0×10^{-6}	1.5×10^{-6}
Gold plate on copper	1.4×10^{-7}	5.7×10^{-8}
Gold plate, untouched for 3 weeks	1.06×10^{-6}	4.3×10^{-7}
Indium on copper	2.0×10^{-7}	1.0×10^{-7}
Silver and gold	2.8×10^{-7}	1.3×10^{-7}

Holm and Meisner (29) report for

Au-Au $(3.7\text{-}10.6)\times10^{-9}\Omega cm^2$	at 38000 psi
Sn-Sn $(7.8\text{-}35)\times10^{-9}\Omega cm^2$	at 78000 psi
Pt-Pt$^+$ 0.3×10^{-9} cm^2	at 380000 psi

$^+$This Pt had been very carefully outgassed prior to the test.

Other materials that have been used for superconducting switches are: in ref (30) Nb-Babbit (4.5%Sn, 1.5%Sb, 85%Pb), in ref(31) Pb, Nb, $NbSn_3$ in different combinations. For scrapped Pb contacts $6.4\times10^{-8}\Omega cm^2$ was obtained at 1125 psi.

1.5 Components of the Resistance.

The resistance between two stabilized superconductors consist of three parts. First the resistance of the interface between superconductor and copper. Second the resistance of the coppermatrix itself. The third contribution is that due to the surface resistance. Plating the surface introduces two additional components: the resistance of the interface between the copper and the plating and the resistance of the plating itself. This does not contribute significantly to the total resistance.

The interface resistance can be reduced by annealing (31). Heat treatment at 500C reduces the interface resistance significantly. Elevation of the annealing temperature above 700° must be avoided as it leads to the

formation of an intermetallic compound (CuTi) with abrupt rise in the resistance. Interface resistance of the order of $1x10^{-8}\Omega cm^2$ were reported. A more recent study (32) shows that samples constructed of very fine filaments have a transverse resistivity in the range of a few $10^{-9}\Omega m$, which is much higher than the resistivity of the copper matrix itself. This resistivity decreases as the filament diameter increases.

The resistance of the copper matrix itself is negligible in most cases. Data about the resistance of copper at low temperature, and different magnetic fields can be found in (33) (34).

The contact resistance depend very much on the mechanical properties of the material and the electrical properties of its oxides, and eventually sulfides. The best results hitherto were obtained with Ag.

2. Conclusion

We are confident that, with silverplated surfaces, we can achieve a joint with $\sigma = 1.5x10^{-9}\Omega cm^2$, carrying $2000A/cm^2$. The applied pressure was 24000 psi or 1700 kg/cm^2. It would be interesting to look at pressures between 24000 psi, and 4000 psi (measurements made by Zar) in order to see whether the resistivity does indeed follows a logarithmic dependence with pressure.

APPENDIX A

An excellent introduction to the subject is

1. A.W.B. Taylor, "Superconductivity", Wykeham Publications (London) LTD, London & Winchester 1970.

With an emphasis on the applications we have

2. V.L. Newhouse , "Applied Superconductivity", John Wiley & Sons, Inc., New York 1964.

Focusing almost entirely on the applications is

3. David Fishlock, "A Guide to Superconductivity", MacDonald, London and America Elsevier Inc., New York, 1969.

Keeping an equilibrium between the scientific theories and the applications

4. M.H. Cohen, "Superconductivity in Science and Technology", University of Chicago Press, Chicago & London, 1968.

A comprehensive and authoritative book with less emphasis on the applications is

5. D. Shoenberg, "Superconductivity", Cambridge University Press, 1965.

Appendix A (cont'd)

Looking more into the physics and the theories are

6. E.A. Lynton, "Superconductivity", New York: John Wiley & Sons, Inc., 1962.

7. J.R. Schrieffer, "Theory of Superconductivity", W.A. Benjamin, In, Reading MA, 1964.

Extensive works on the subject are

8. S. Foner, B.B. Schwartz, "Superconducting Machines and Devices, Large Systems Applications", Plenum Press, New York-London 1973.

9. Gregory, Mathews, Edelsok, "The Science & Technology of Superconductors, Vol. 1, 2", Plenum Press, New York-London 1973.

REFERENCES

1. "Superconductive Performance of Production NbTi Alloys", D.A. Colling, T.A. deWinter, W.C. McDonald, W.C. Turner, IEEE Transaction on Magnetics, Vol. MAG-13, no. 1, January 1977.

2. "The Critical Current Density of Nb-Ti, Superconductor in the Temperature Range 1.9 to 4.2K", P.E. Hanley and M.N. Biltcliffe, Proceedings of the 4th Inst. Cryogenic Conference, Eindhoven 24/26 May 1972, IPC Science & Technology Press.

3. "Development of Multifilamentary Nb_3Sn conduction for Fusion Research", D.N. Cornish D.W. Deis, R.L. Nelson, R.M. Scanlan, C.E. Taylor, R.R. Vandervoort,F.J. Wittmayer, J.P. Zbasnik, IEEE Transactions on Magnetics, Vol MAG-13, No. 1, January 1977.

4. "Further Developments in Stabilized Multifilamentary Nb_3Sn Superconductors, E. Adam, E. Gregory, F.T. Ormand, IEEE Transactions on Magnetics, Vol. MAG-13, No. 1, January 1977.

5. "Large-scale Applications of Superconductivity", Brian B. Schwartz, Simon Foner, Physics Today, July 1977, Vol. 30 no. 7.

6. "Superconducting Magnets in the World of Energy, Especially in Fusion Power, P. Komarek, Cryogenics, March 1976.

7. "A Method for Studying the Electrical Properties of Specimens in the Pressure Region up to 300 kbar and at Temperatures from 0.1 to 200K", N.B. Brandt, I.V. Berman, Yu. P. Kurkin, and V.I. Sidorov, Cryogenics, January 1976.

8. "Stabilization of Superconductors for use in Magnets", Martin N. Wilson, IEEE Transactions on Magnetics, Vol. MAG-13, no. 1, January 1977.

9. "Development Program for MHD Power Generation, Superconducting Magnet Study", Final Report, Vol. IV. Contract No. E(49-18)-2015, A.M. Hatch, R.C. Beals, A.J. Sofia, Avco Research Laboratories, April 1977.

10. Patent 3,422,529 "Method of Making a Superconductive Joint", J.M. Nuding, filed December 9, 1963.

11. Superconducting Joint Behavior Multifilamentary Wires, "Joint-making and Joint Results", M.J. Leupold and Y. Iwasa, Cryogenics, April 1976.

12. Patent 3,527,876 "Electrical Connection Between Superconductors", E. Karvonen, et al, filed Sept. 23, 1968.

13. "Superconducting Joint Between Multifilamentary Wires", G. Luderer, P. Dullenkopf, G. Laukien Cryogenics, September 1974.

14. Patent 3,453,378 "Superconductive Joint", A.D. McInturff, filed January 19, 1967.

15. "Joining NbTi Superconductors by Ultrasonic Welding", J.W. Hafstrom, D.H. Killpatrick, R.C. Niemann, J.R. Purcell, H.R. Thresh, IEEE Transactions on Magnetics, Vo. MAG-13, no. 1, January 1977.

16. "Explosive Joints in Nb-Ti/Cu Composite Superconductors", D.N. Cornish and J.P. Zbasnik, H.E. Pattee, Proceedings of the Sixth Symp. on Engineering Problems of Fusion Research, San Diego, California, Nov. 18-21, 1975, IEEE Publication no.75CH 1097-5-NPS.

17. "Superconductor Joining Methods for Large CTR Magnets", P.M. Rackov, C.D. Henning, Proceedings of the Sixth Symp. on Engineering Problems of Fusion Research, San Diego, California, Nov. 18-21, 1975, IEEE Publication no. 75CH1097-5-NPS.

18. "Electrical Switch Contact Resistance at 4.2K", J.L. Zar., proceedings of the 1967 Cryogenic Eng. Conf., August 21-23, Stanford, K.D. Zimmerhaus Editor, Plenum Press.

19. "A Remotely Operated Electromechanical Cryogenic Switch, 100A 1μΩ to Infinite Resistance", P. Krueger, Proceedings of the 4th Int. Cryogenic Engineering Conference, Eindhoven 24/26 May 1972, IPC Science and Technology Press.

20. "Progress in Switching Technology for Mets Systems", E.M. Honig, C.E. Swannack, R.W. Warren, D.H. Whitaker, 1976 IEEE International Conference on Plasma Science, May 24-29, 1976 at the University of Texas at Austin, Austin, Texas.

21. "Electrical Measurements and Measuring Instruments", Golding, Pitman Paperbacks 1968.

22. "Electrical Resistance of Metals", George Terence Meaden, Plenum Press, New York 1965.

23. "Measurement of Electrical Resistivity of Bulk Metal", J.E. Zimmerman, The Review of Scientific Instruments, Volume 32, Number 4, April 1961.

24. "A New Arrangement of the Induction Method of Measuring Electrical Conductivity", V.I. Khotkevich, M. Ya Zabara, Cryogenics, March 1963.

25. "Eddy-Current Method for Measuring the Resistivity of Metals", C.R. Bean, R.W. DeBlois, L.B. Nesbitt, Journal of Applied Physics, vol. 30, no. 12, December 1959.

26. "Superconducting Joint Between Multifilamentary Wires", 2. Joint Evaluation Technique, Y. Iwasa, Cryogenics, April 1976.

27. Y. Iwasa, Private Communication, Experiments made at NML in 1975.

28. D. Hay, Private Communication, Experiments Made at CERN in 1971.

29. "Messungen mit Hilfe von flüssigem Helium XIII. Kontaktwiderstand zwischen Supraleitern und Nichtsupraleitern," R.Holm, W. Meissner, Zeitschrift für Physik, Bd 74, 1932, p. 715-735.

30. "A Mechanical Superconducting Switch for Low Temperature Instrumentation", J.D. Siegwarth, D.B. Sullivan, Rev. of Sci. Inst., Volume 43, no. 1, January 1973.

31. "Contact Resistance of Stabilized Superconducting Wires", Y. Furuto, M. Ikeda, 2nd European Cryogenic Eng. Conference. May 7-10, 1968, J.P. Ray Editor, Iliffe Science and Technology Publications Ltd., Surrey, England

32. "Transverse Resistivity in Multifilament Superconductive Composites ", B. Turck, M. Wake, M. Kobayashi, Cryogenics, April 1977.

33. "Magnetic Resistance of Copper at 4.2k in Transverse Fields up to 100 kG", M.G. Benz, Journal of Applied Physics, Vol. 40, no. 3, April 1969.

34. "A Simple Method for Producing High Conductivity Copper for Low Temperature Application " S.S. Rosenblum, W.A. Steyert, F.R. Ficket, Cryogenics, November 1977.